Contact mechanics and elements of tribology

Lecture 6.

Roughness and coupled problems

Vladislav A. Yastrebov

MINES ParisTech, PSL Research University, Centre des Matériaux, CNRS UMR 7633, Evry, France

@ Centre des Matériaux
February 11, 2016

Roughness

- **Natural and industrial surfaces are *rough*:**
  - processing
  - polishing
  - coating
  - microstructure
  - surface energy
  - deformation
  - aging
  - environment

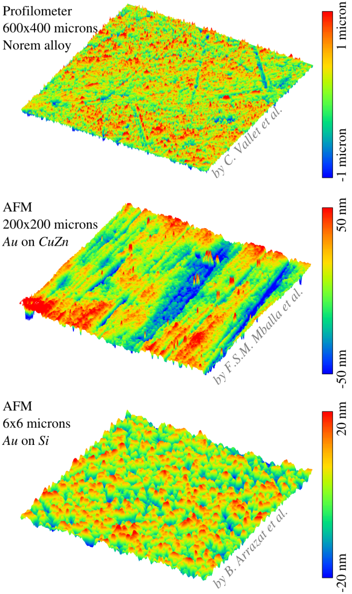

Fig. Examples of rough surfaces

Roughness

- **Natural and industrial surfaces are *rough*:**
  - processing
  - polishing
  - coating
  - microstructure
  - surface energy
  - deformation
  - aging
  - environment

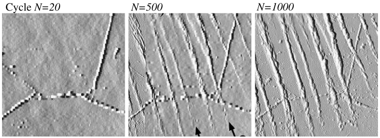

Fig. Persistent slip marks [1]

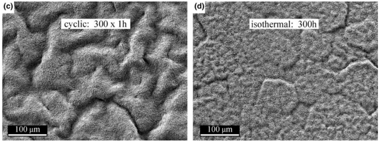

Fig. Rumpling (thermal cycling induced roughness in air)[2]

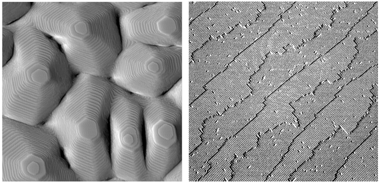

Fig. Epitaxial surface growth [3,4]

[1] J.Polák, J. Man & K. Orbtlík, Int J Fatigue 25 (2003)
[2] V.K. Tolpygo, D.R. Clarke, Acta Mat 52 (2004)
[3] M. Einax, W. Dieterich, P. Maass, Rev Mod Phys 85 (2013)
[4] J.R. Arthur, Surf Sci 500 (2002)

Roughness

- **Natural and industrial surfaces are *rough*:**
  - processing
  - polishing
  - coating
  - microstructure
  - surface energy
  - deformation
  - aging
  - environment
- **Roughness affects:**
  - stress-strain state
  - dry friction
  - wear
  - adhesion
  - fluid flow
  - sealing
  - energy transfer

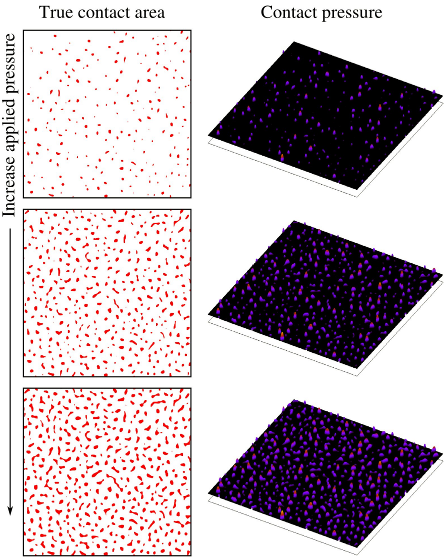

Fig. True contact area and stress fluctuations

Roughness

- **Natural and industrial surfaces are *rough*:**
  - processing
  - polishing
  - coating
  - microstructure
  - surface energy
  - deformation
  - aging
  - environment
- **Roughness affects:**
  - stress-strain state
  - dry friction
  - wear
  - adhesion
  - fluid flow
  - sealing
  - energy transfer

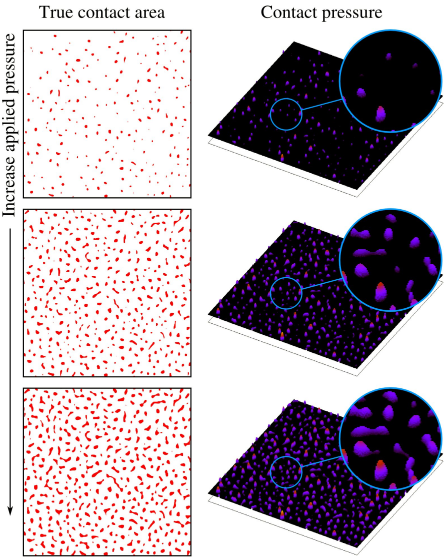

Fig. True contact area and stress fluctuations

Roughness

- **Natural and industrial surfaces are *rough*:**
  - processing
  - polishing
  - coating
  - microstructure
  - surface energy
  - deformation
  - aging
  - environment
- **Roughness affects:**
  - stress-strain state
  - dry friction
  - wear
  - adhesion
  - fluid flow
  - sealing
  - energy transfer

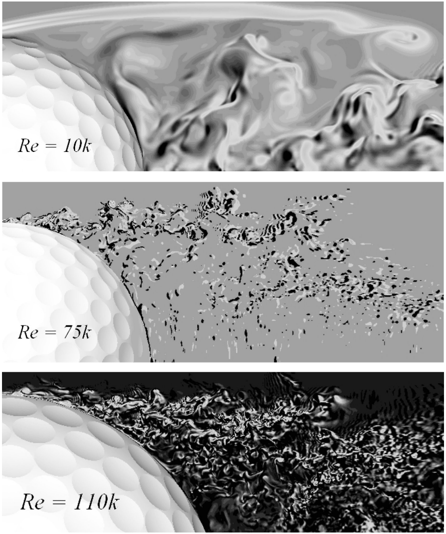

Fig. Numerical simulation of airflow around a (dimpled) golf ball [5]

[5] C.E. Smith, PhD thesis (2011)

Roughness

- **Natural and industrial surfaces are *rough*:**
  - processing
  - polishing
  - coating
  - microstructure
  - surface energy
  - deformation
  - aging
  - environment
- **Roughness affects:**
  - stress-strain state
  - dry friction
  - wear
  - adhesion
  - fluid flow
  - sealing
  - energy transfer

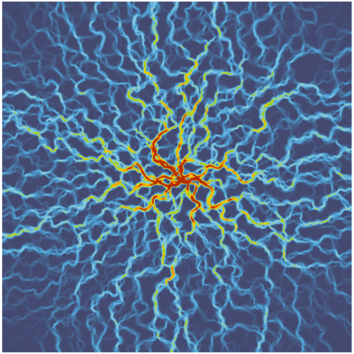

Fig. Fluid passage through free volume between rough surfaces

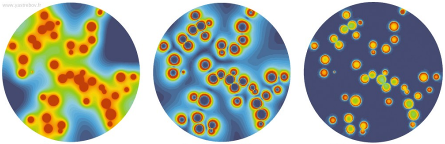

Fig. Heat transfer between rough surfaces (asperity-based model)

Multiscale and multiphysical contact

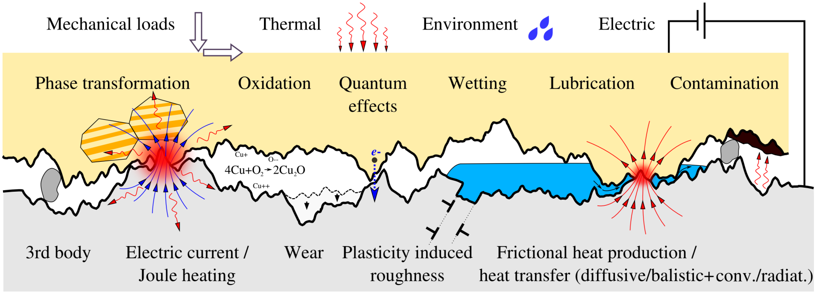

- Roughness scale
- Two different materials (with microstructures)
- Two different roughness

Multiscale and multiphysical contact

Plasticity induced roughness
Dislocation traces
Phase transformations
Visco-plasticity
Fracture / wear

Roughness

Characterisation & modeling

Contamination
Corrosion
Electromigration
Convection
Tunneling

Mechanics

Scale-relevant material and interface models

Strong coupling

Other physics

All phenomena described by other equations

Tribology
wear, adhesion, 3rd body

Transport
thermal, electric, fluid

Tribology
lubrication

Environment & chemistry
oxidation, corrosion

Metallurgy
phase transformations

Multiscale and multiphysical contact

Roughness

Isotropic, Gaussian, self-affine

Mechanics

Linear elasticity
Frictionless and non-adhesive contact

Weak coupling

Other physics

Fluid transport
for incompressible fluid

Multiscale and multiphysical contact

Roughness 1

Isotropic, Gaussian, self-affine

Mechanics 2

Linear elasticity
Frictionless and non-adhesive contact

Weak coupling

Other physics 3

Fluid transport
for incompressible fluid

Multiscale and multiphysical contact

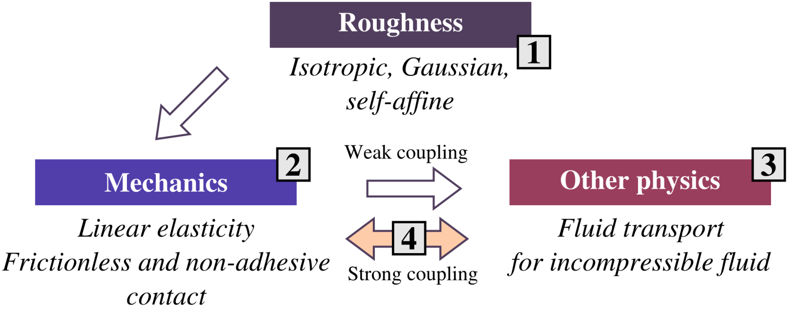

Roughness. Characteristics.

- Fractal (self-affine) roughness
- Power spectral density (PSD)

  $$\Phi(k) \sim k^{-2(H+1)}$$

  k is a wavenumber,
  H is the Hurst exponent.
- **Isotropic**/anisotropic surfaces
- **Gaussian**/non-Gaussian height distribution $P(h)$

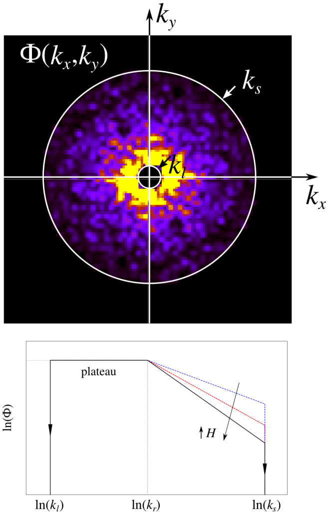

Fig. 3D and radial power spectral densities

Roughness. Characteristics.

- Fractal (self-affine) roughness
- Power spectral density (PSD)

  $$\Phi(k) \sim k^{-2(H+1)}$$

  k is a wavenumber,
  H is the Hurst exponent.
- **Isotropic**/anisotropic surfaces
- **Gaussian**/non-Gaussian height distribution $P(h)$

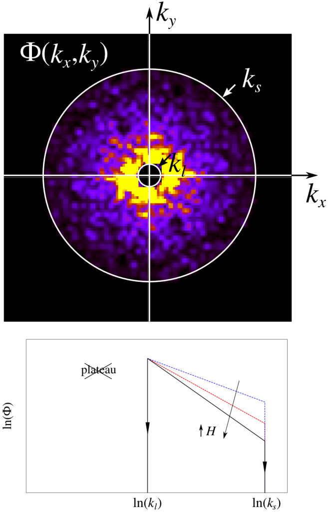

Fig. 3D and radial power spectral densities

Roughness. Characteristics.

- Fractal (self-affine) roughness
- Power spectral density (PSD)

  $$\Phi(k) \sim k^{-2(H+1)}$$

  k is a wavenumber,
  H is the Hurst exponent.
- **Isotropic**/anisotropic surfaces
- **Gaussian**/non-Gaussian height distribution $P(h)$

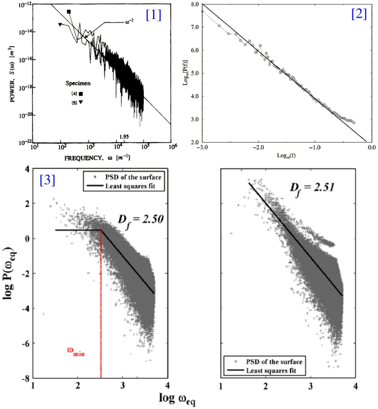

Fig. Power spectral density, measurements

[1] Majumdar, Tien, Wear 136 (1990)
[2] Schmittbuhl, Jørgen Måløy, Phys. Rev. Lett. 78 (1997)
[3] Vallet, Lasseux, Sainsot, Zahouani, Tribol. Int. 42 (2009)

Roughness. Characteristics.

- Fractal (self-affine) roughness
- Power spectral density (PSD)

  $$\Phi(k) \sim k^{-2(H+1)}$$

  k is a wavenumber,
  H is the Hurst exponent.
- **Isotropic**/anisotropic surfaces
- **Gaussian**/non-Gaussian height distribution $P(h)$

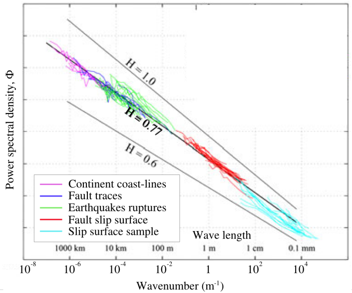

Fig. Power spectral density, geological scales

Adapted from
[4] Renard, Candela, Bouchaud, Geophys. Res. Lett. 40 (2013)

Roughness. Characteristics.

- Fractal (self-affine) roughness
- Power spectral density (PSD)

$$\Phi(k) \sim k^{-2(H+1)}$$

  k is a wavenumber,
  H is the Hurst exponent.
- **Isotropic**/anisotropic surfaces
- **Gaussian**/non-Gaussian height distribution $P(h)$

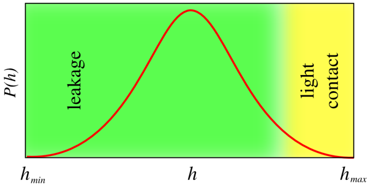

Fig. Height distribution $P(h)$

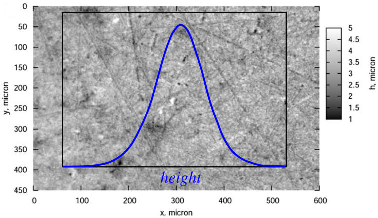

Fig. Height distribution of a polished metal surface

Roughness. Characteristics.

- Fractal (self-affine) roughness
- Power spectral density (PSD)

  $$\Phi(k) \sim k^{-2(H+1)}$$

  k is a wavenumber,
  H is the Hurst exponent.
- **Isotropic**/anisotropic surfaces
- **Gaussian**/non-Gaussian height distribution $P(h)$
- **Characteristics:**
  - $\sqrt{\langle h^2 \rangle}$ - *rms heights*
  - $\sqrt{\langle |\nabla h|^2 \rangle}$ - *rms slope (surface gradient)*
  - $\alpha = m_{00} m_{40} / m_{20}^2$ - *breadth of the spectrum (Nayak's parameter*[B]*),*

  spectral moments $m_{pq} = \iint\limits_{-\infty}^{\infty} k_x^p k_y^q \Phi(k_x, k_y)\, dk_x dk_y$
- **Random process theory**

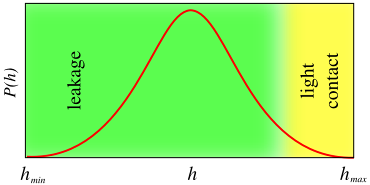

Fig. Height distribution $P(h)$

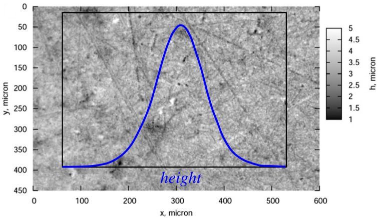

Fig. Height distribution of a polished metal surface

[A] Longuet-Higgins, Philos. Trans. R. Soc. A 250:157 (1957)
[B] Nayak, J. Lub. Tech. (ASME) 93:398 (1973)
[C] Greenwood, Wear 261: 191 (2006)
[D] Borri, Paggi, J. Phys. D Appl Phys 48:045301 (2015)

Roughness. Characteristics.

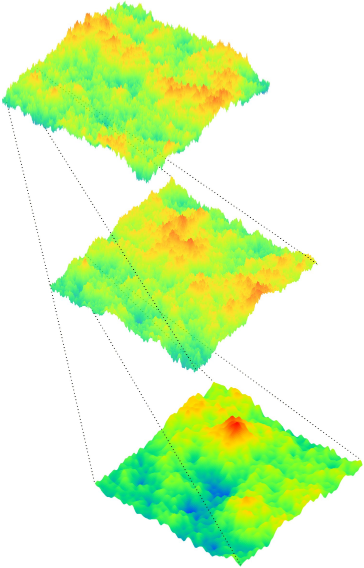

Fig. Example of a rough surface for $H = 0.3$

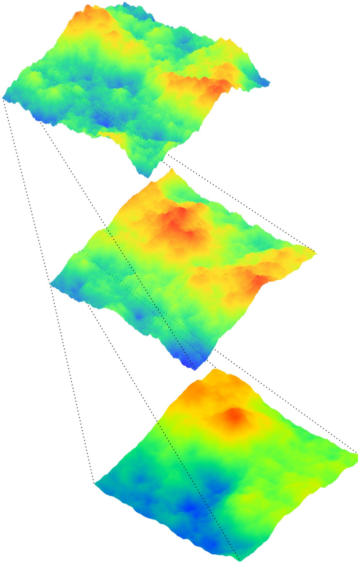

Fig. Example of a rough surface for $H = 0.8$

Recall: the Hurst exponent H and the fractal dimension D in 2D space are interconnected via $D = 3 - H$

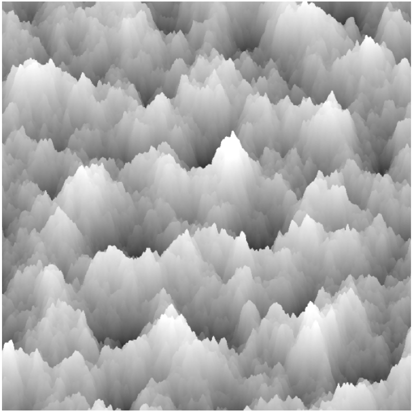

Flight over a rough surface

Fractals

Romanesco broccoli www.fourmilab.ch

Fractals

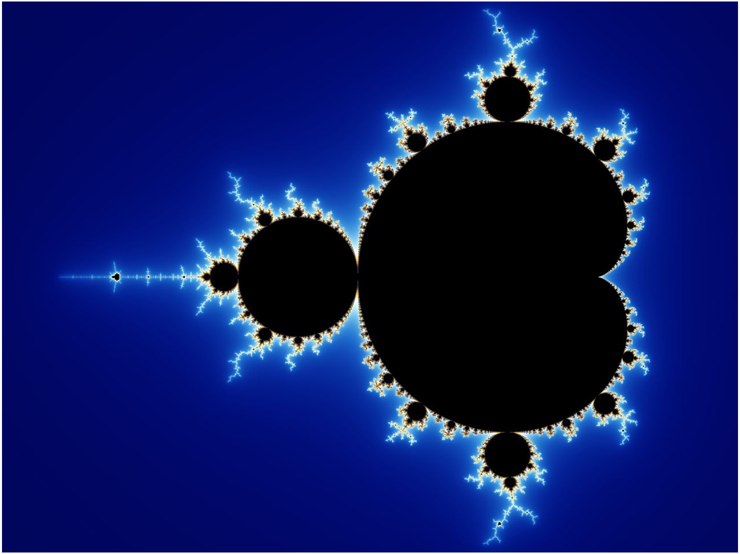

Mandelbrot set (Wikipedia)

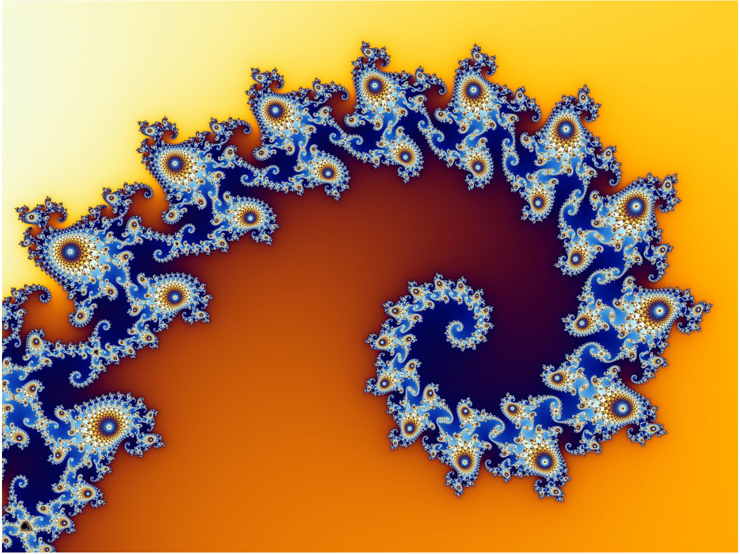

Element of Mandelbrot set (Wikipedia)

Fractals

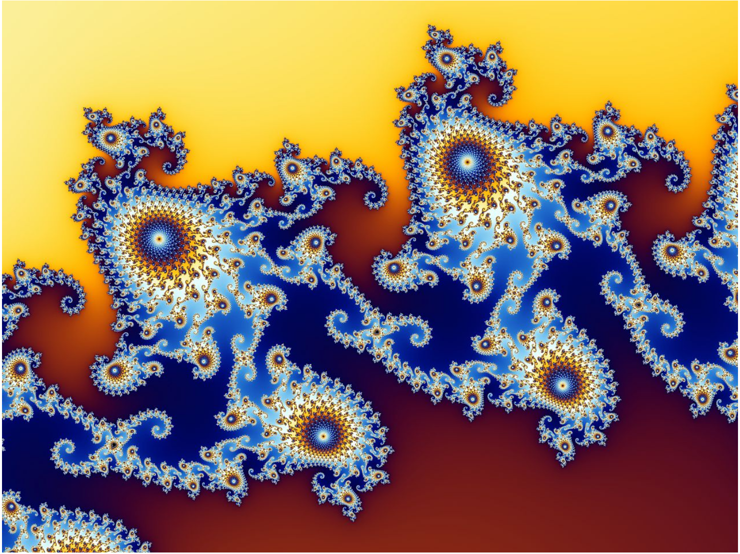

Element of Mandelbrot set (Wikipedia)

Fractals

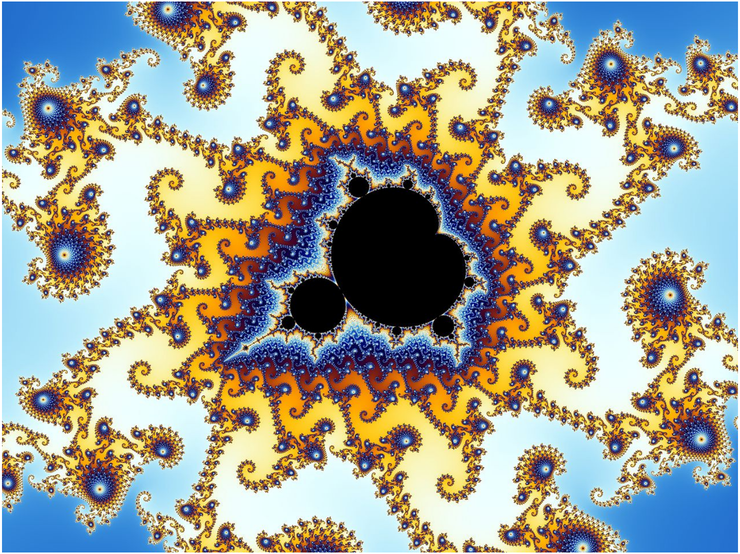

Element of Mandelbrot set (Wikipedia)

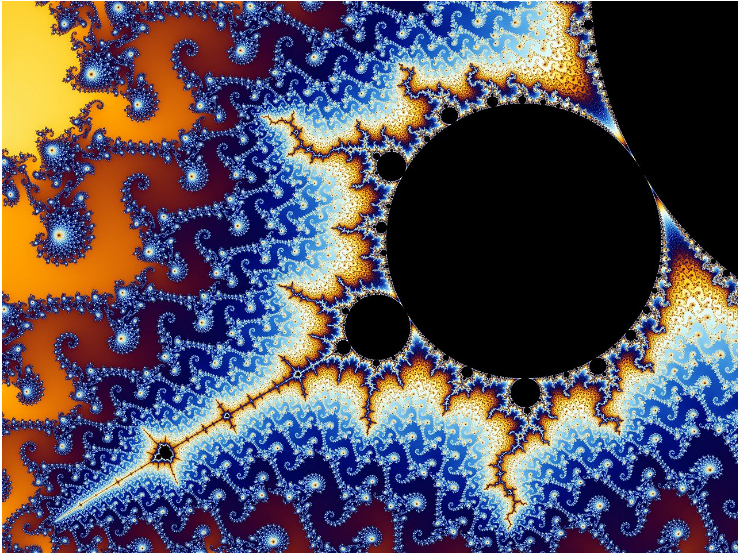

Element of Mandelbrot set (Wikipedia)

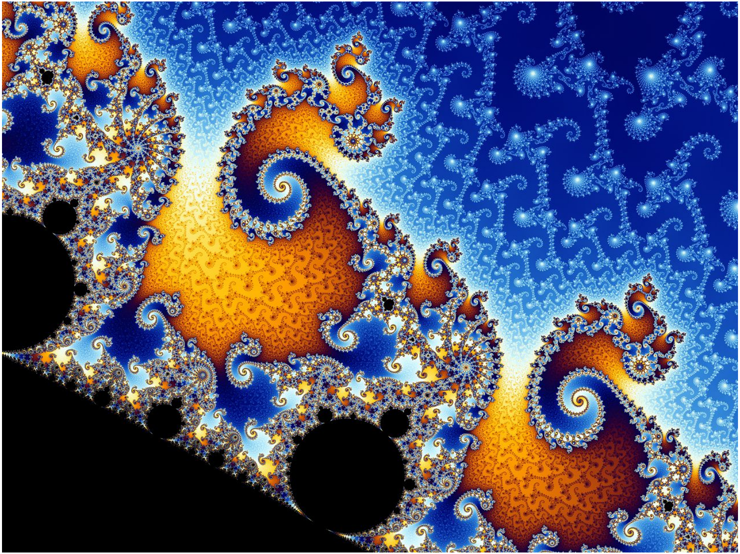

Element of Mandelbrot set (Wikipedia)

Animation

Synthesized rough surfaces

Real space | **Fourier space**

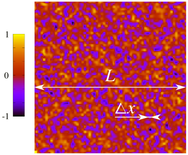

White noise, r_{ij}

[1] Y. Z. Hu and K. Tonder, Int. J. Machine Tools Manuf. 32, 83 (1992)

Synthesized rough surfaces

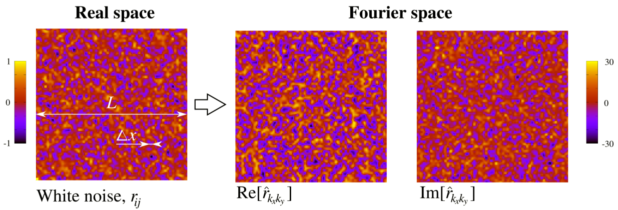

[1] Y. Z. Hu and K. Tonder, Int. J. Machine Tools Manuf. 32, 83 (1992)

Synthesized rough surfaces

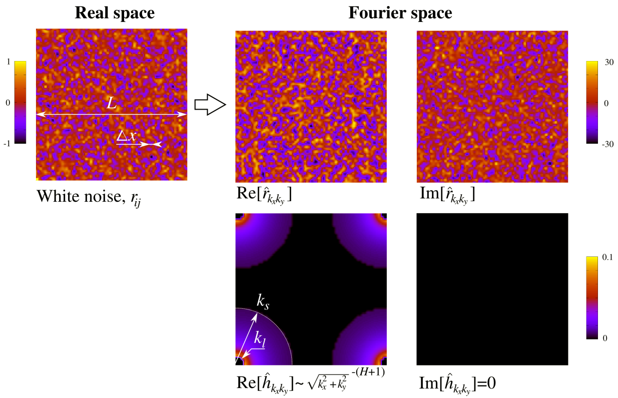

[1] Y. Z. Hu and K. Tonder, Int. J. Machine Tools Manuf. 32, 83 (1992)

Synthesized rough surfaces

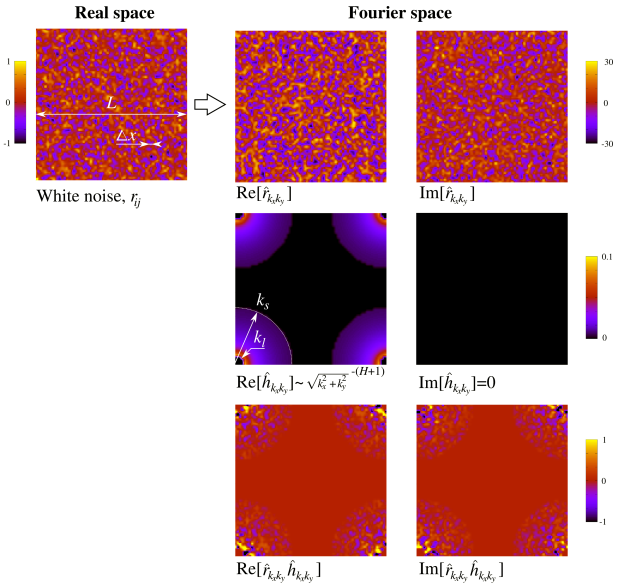

[1] Y. Z. Hu and K. Tonder, Int. J. Machine Tools Manuf. 32, 83 (1992)

Synthesized rough surfaces

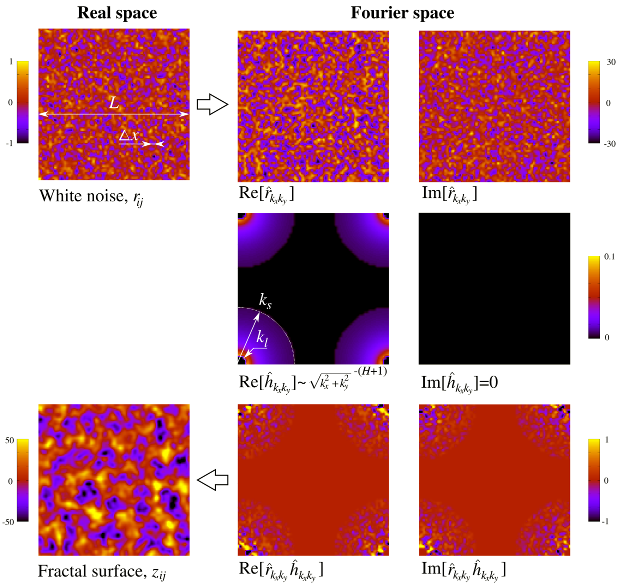

[1] Y. Z. Hu and K. Tonder, Int. J. Machine Tools Manuf. 32, 83 (1992)

- Effect of the high frequency cutoff k_s

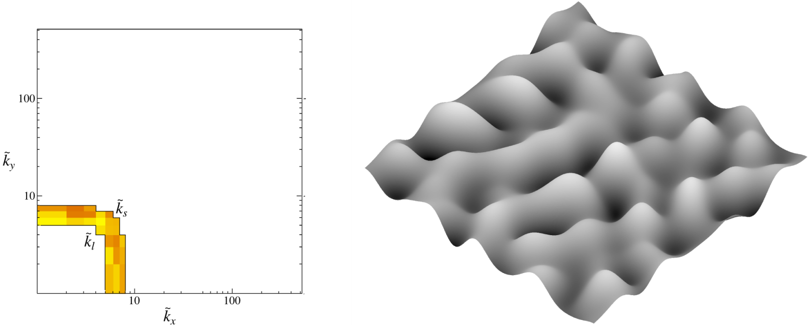

Fig. Power spectral density (Fourier space)
and corresponding rough surface (real space) for
$k_l = 4, \quad k_s = 8$

- Effect of the high frequency cutoff k_s

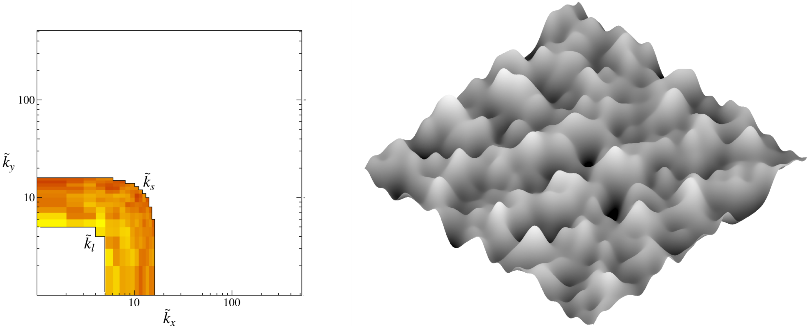

Fig. Power spectral density (Fourier space)
and corresponding rough surface (real space) for
$k_l = 4, \quad k_s = 16$

- Effect of the high frequency cutoff k_s

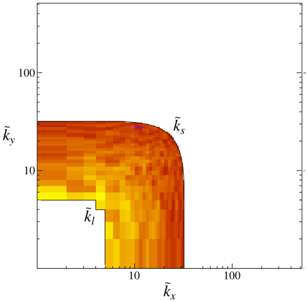

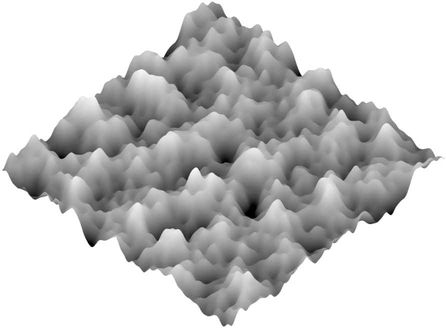

Fig. Power spectral density (Fourier space)
and corresponding rough surface (real space) for
$k_l = 4, \quad k_s = 32$

- Effect of the high frequency cutoff k_s

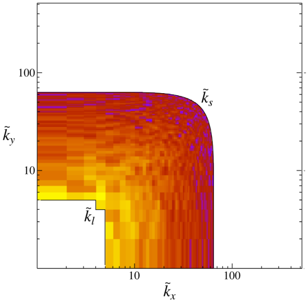

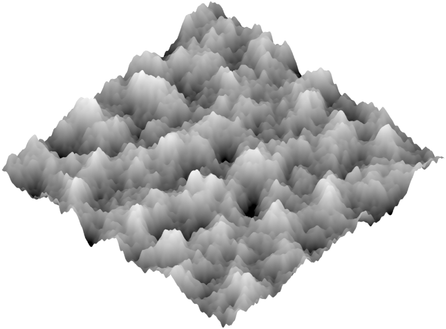

Fig. Power spectral density (Fourier space)
and corresponding rough surface (real space) for
$k_l = 4, \quad k_s = 64$

- Effect of the high frequency cutoff k_s

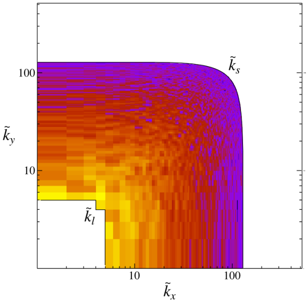

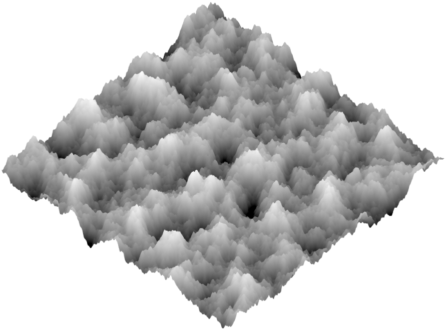

Fig. Power spectral density (Fourier space)
and corresponding rough surface (real space) for
$k_l = 4, \quad k_s = 128$

- Effect of the lower frequency cutoff k_l for $k_s/k_l = \text{const}$

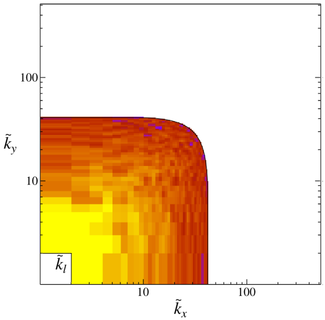

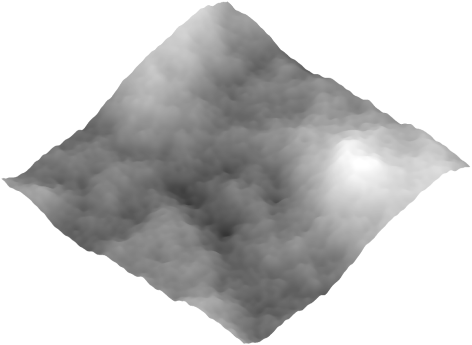

Fig. Power spectral density (Fourier space) and corresponding rough surface (real space) for
$k_l = 1, \quad k_s = 43$

Effect of parameters: illustration

- Effect of the lower frequency cutoff k_l for $k_s/k_l = \text{const}$

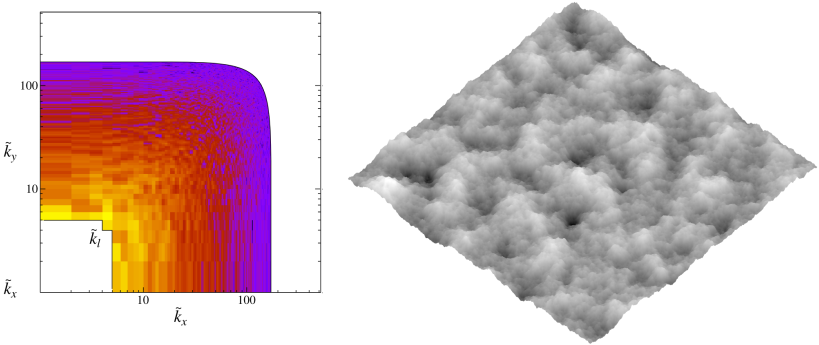

Fig. Power spectral density (Fourier space)
and corresponding rough surface (real space) for
$k_l = 4, \quad k_s = 171$

Effect of parameters: illustration

- Effect of the lower frequency cutoff k_l for $k_s/k_l = \mathrm{const}$

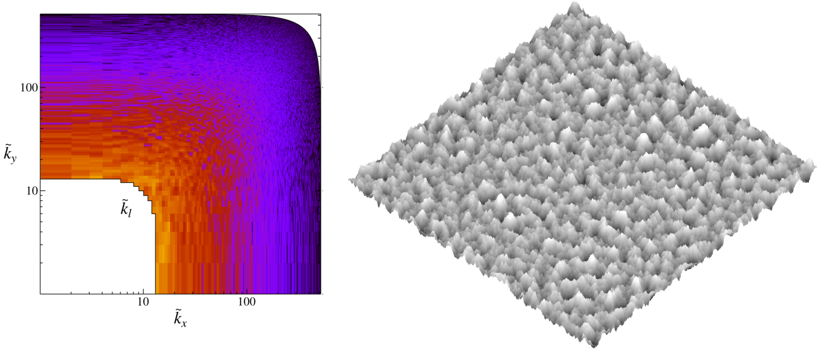

Fig. Power spectral density (Fourier space)
and corresponding rough surface (real space) for
$k_l = 12, \quad k_s = 512$

- Effect of the ratio of the higher cutoff to the discretization k_s/N

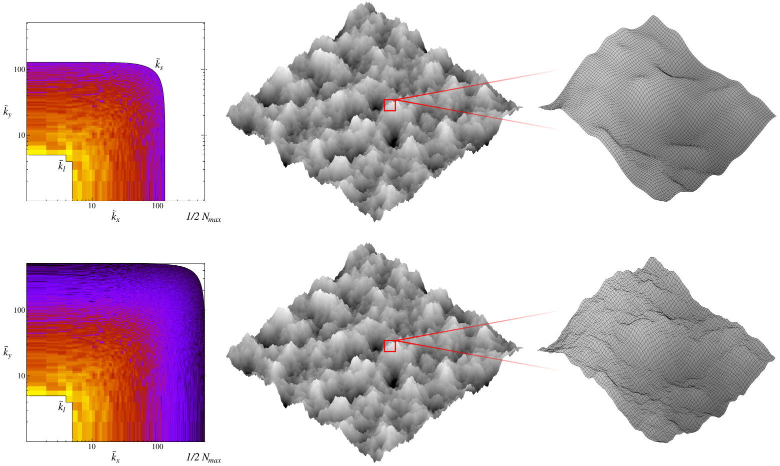

Fig. Power spectral densities (Fourier space)
and corresponding rough surfaces (real space) for
$k_l = 12, \quad k_s/N = 1/8$ **VS** $k_l = 12, \quad k_s/N = 1/2$

Effect of parameters: illustration

- Effect of the ratio of the higher cutoff to the discretization k_s/N

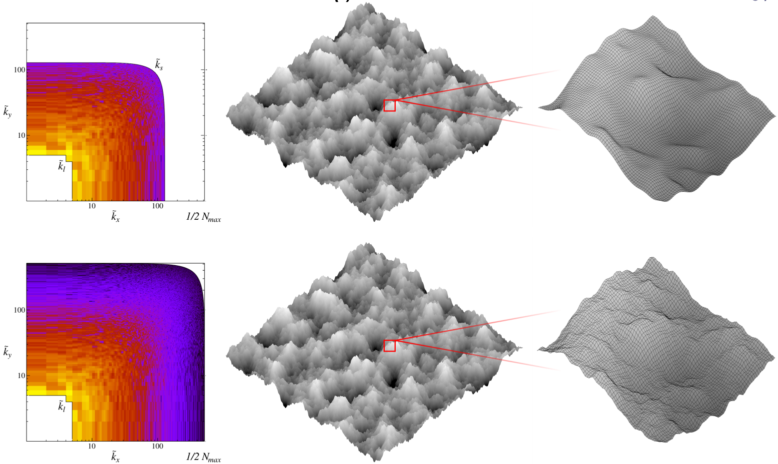

Fig. Power spectral densities (Fourier space)
and corresponding rough surfaces (real space) for
$k_l = 12,\quad k_s/N = 1/8$ **(fine)** **VS** $k_l = 12,\quad k_s/N = 1/2$ **(too coarse)**
for mechanical simulations

- Effect of the discretisation (single asperity)

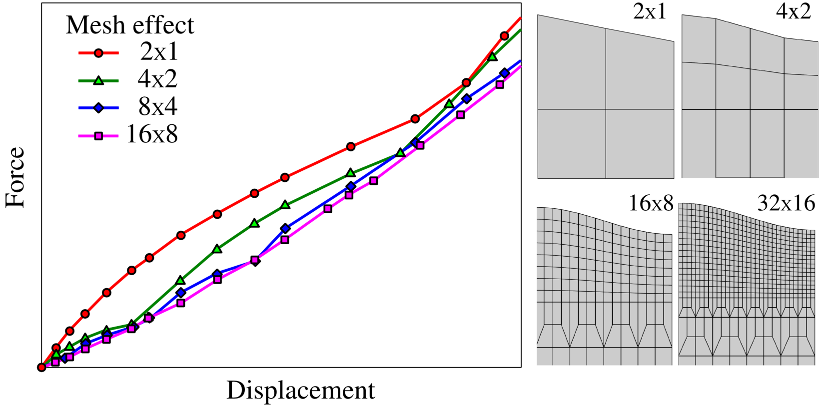

Fig. Effect of the mesh on mechanical response

Effect of parameters: illustration

- Data interpolation (Shanon, bi-cubic Bézier surfaces)

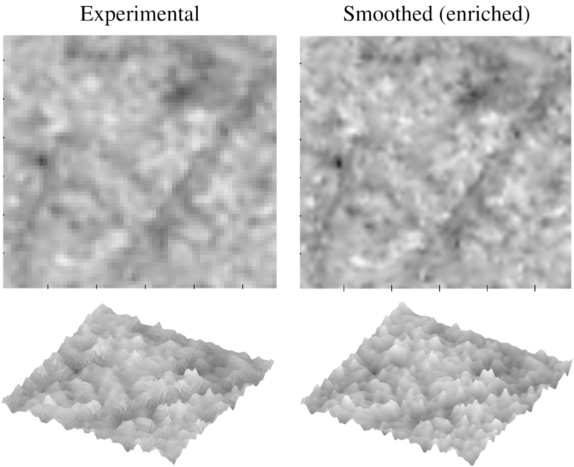

Fig. Bi-cubic Bézier interpolation of an experimental rough surface

[1]Hyun, Robbins, Tribol. Int. (2007)
[2] Yastrebov, Durand, Proudhon, Cailletaud, C.R. Mécan. (2011)

Effect of parameters:

- k_l low frequency cutoff
  - representativity/normality[1,2,3]
- k_s high frequency cutoff
  - smoothness and density of asperities
- $\zeta = k_s/k_l$ ratio[3]
  - breadth of the spectrum

$$\boxed{\alpha \sim \zeta^{2H}}$$

Nayak's parameter α is the central characteristic of roughness in asperity based mechanical models.

[1] Vallet, Lasseux, Sainsot, Zahouani, Tribol. Int. (2009)
[2] Yastrebov, Durand, Proudhon, Cailletaud, C.R. Mécan. (2011)
[3] Yastrebov, Anciaux, Molinari, Phys. Rev. E (2012)
[4] Yastrebov, Anciaux, Molinari, Int. J. Solids Struct. (2015)

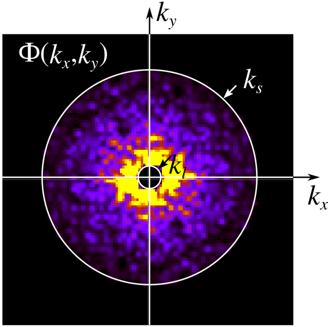

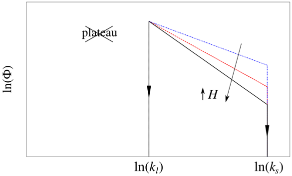

Fig. 3D and radial power spectral densities

Effect of parameters:

- k_l low frequency cutoff
  - representativity/normality[1,2,3]
- k_s high frequency cutoff
  - smoothness and density of asperities
- $\zeta = k_s/k_l$ ratio[3]
  - breadth of the spectrum

$$\boxed{\alpha \sim \zeta^{2H}}$$

Nayak's parameter α is the central characteristic of roughness in asperity based mechanical models.

[1] Vallet, Lasseux, Sainsot, Zahouani, Tribol. Int. (2009)
[2] Yastrebov, Durand, Proudhon, Cailletaud, C.R. Mécan. (2011)
[3] Yastrebov, Anciaux, Molinari, Phys. Rev. E (2012)
[4] Yastrebov, Anciaux, Molinari, Int. J. Solids Struct. (2015)

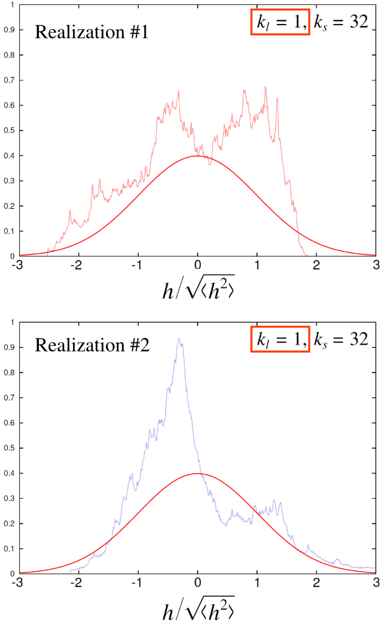

Effect of parameters

Effect of parameters:

- k_l low frequency cutoff
  - representativity/normality[1,2,3]
- k_s high frequency cutoff
  - smoothness and density of asperities
- $\zeta = k_s/k_l$ ratio[3]
  - breadth of the spectrum

$$\boxed{\alpha \sim \zeta^{2H}}$$

Nayak's parameter α is the central characteristic of roughness in asperity based mechanical models.

[1] Vallet, Lasseux, Sainsot, Zahouani, Tribol. Int. (2009)
[2] Yastrebov, Durand, Proudhon, Cailletaud, C.R. Mécan. (2011)
[3] Yastrebov, Anciaux, Molinari, Phys. Rev. E (2012)
[4] Yastrebov, Anciaux, Molinari, Int. J. Solids Struct. (2015)

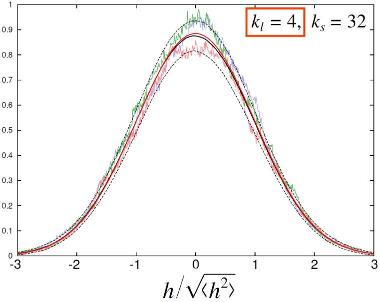

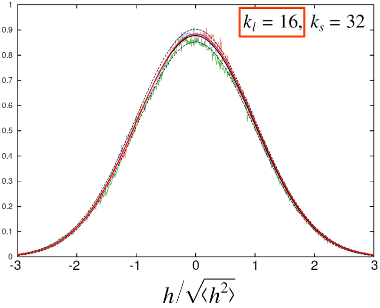

Model and reality

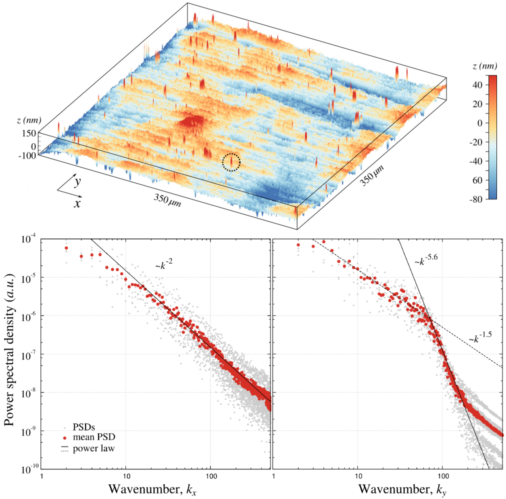

[1] Yastrebov et al, Three-level multi-scale modeling of electrical contacts sensitivity study and experimental validation, Proceedings of Holm Conference, 2015.

Model and reality

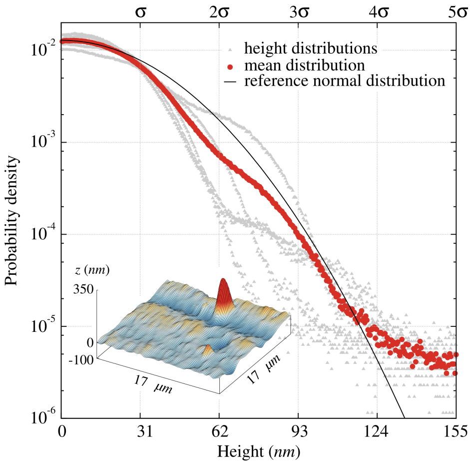

[1] Yastrebov et al, Three-level multi-scale modeling of electrical contacts sensitivity study and experimental validation, Proceedings of Holm Conference, 2015.

- **Real contact area** between rough surfaces in contact increases with applied pressure

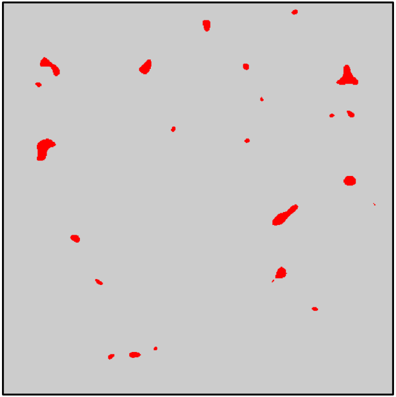

Fig. Real contact area A

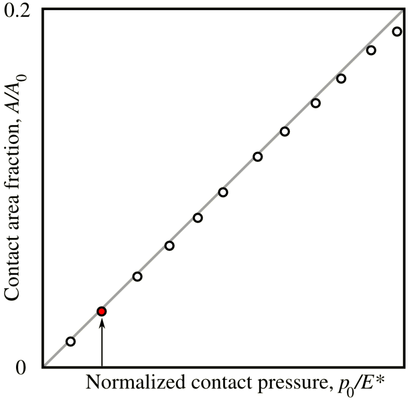

Fig. Real contact area A vs pressure p_0

- **Real contact area** between rough surfaces in contact increases with applied pressure

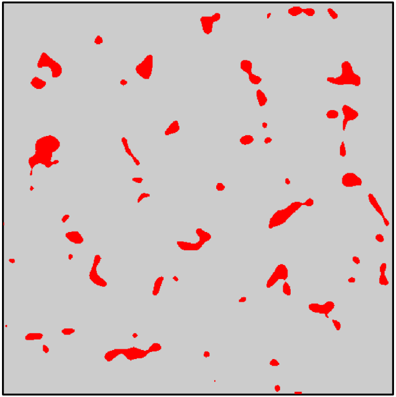

Fig. Real contact area A

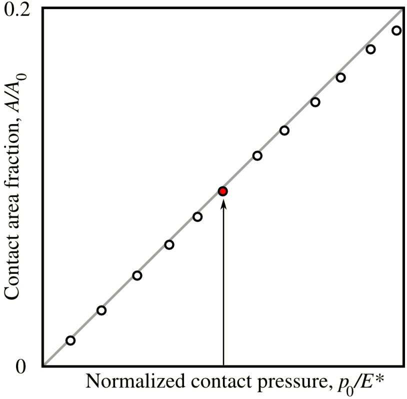

Fig. Real contact area A vs pressure p_0

- **Real contact area** between rough surfaces in contact increases with applied pressure

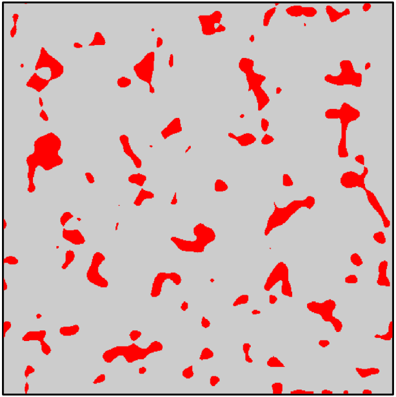

Fig. Real contact area A

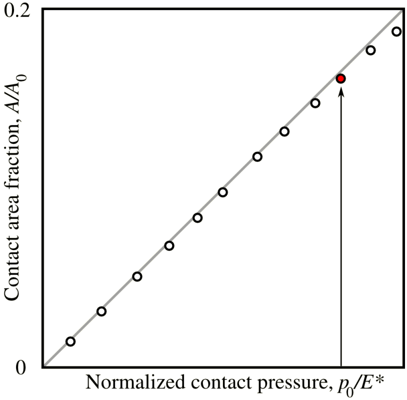

Fig. Real contact area A vs pressure p_0

Asperity based models

[1] Greenwood, Williamson. *P Roy Soc Lond A Mat* (1966)
[2] Bush, Gibson, Thomas. *Wear* (1975)
[3] Mc Cool. *Wear* (1986)
[4] Thomas. *Rough Surfaces* (1999)
[5] Greenwood. *Wear* (2006)
[6] Carbone. *J. Mech. Phys. Solids* (2009)
[7] Ciavarella, Greenwood, Paggi. *Wear* (2008)

Persson's model

[8] Persson. *J. Chem. Phys.* (2001)
[9] Persson. *Phys. Rev. Lett.* (2001)
[10] Persson, Bucher, Chiaia. *Phys. Rev. B* (2002)
[11] Müser. *Phys. Rev. Lett.* (2008)

Cross-link studies

[12] Manners, Greenwood. *Wear* (2006)
[13] Carbone, Bottiglione. *J. Mech. Phys. Solids* (2008)
[14] Paggi, Ciavarella. *Wear* (2010)

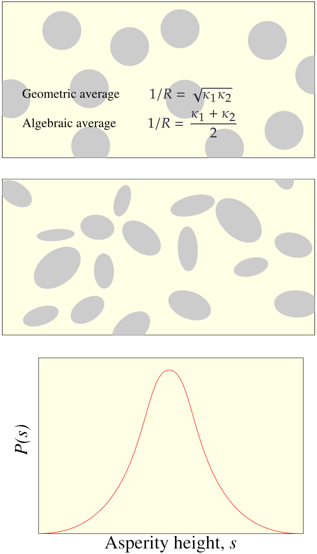

Fig. Asperity based models

Analytical models

Asperity based models

[1] Greenwood, Williamson. *P Roy Soc Lond A Mat* (1966)
[2] Bush, Gibson, Thomas. *Wear* (1975)
[3] Mc Cool. *Wear* (1986)
[4] Thomas. *Rough Surfaces* (1999)
[5] Greenwood. *Wear* (2006)
[6] Carbone. *J. Mech. Phys. Solids* (2009)
[7] Ciavarella, Greenwood, Paggi. *Wear* (2008)

Persson's model

[8] Persson. *J. Chem. Phys.* (2001)
[9] Persson. *Phys. Rev. Lett.* (2001)
[10] Persson, Bucher, Chiaia. *Phys. Rev. B* (2002)
[11] Müser. *Phys. Rev. Lett.* (2008)

Cross-link studies

[12] Manners, Greenwood. *Wear* (2006)
[13] Carbone, Bottiglione. *J. Mech. Phys. Solids* (2008)
[14] Paggi, Ciavarella. *Wear* (2010)

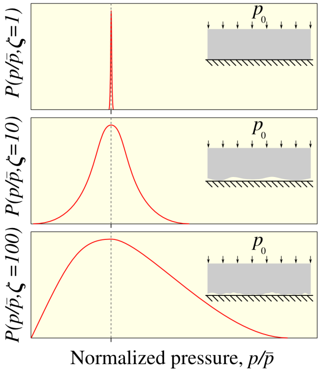

Fig. Persson's model

$$\boxed{\frac{\partial P(p,\zeta)}{\partial V(\zeta)} = \frac{1}{2}\frac{\partial^2 P(p,\zeta)}{\partial p^2}} \qquad P(0,\zeta) = 0$$

$$V(\zeta) = \tfrac{1}{2}E^* m_2(\zeta) = \tfrac{\pi E^*}{2}\int\limits_{k_l}^{\zeta k_l} k^3 \Phi^p(k)\,dk$$

Asperity based models — **Persson's model**

1. Evolution of the real contact area $A(p_0)$ for $A/A_0 \to 0$

$$\boxed{\frac{A}{A_0} = \frac{\kappa}{\sqrt{\langle|\nabla h|^2\rangle}} \frac{p_0}{E^*}}$$

$\kappa_{\mathrm{BGT}} = \sqrt{2\pi} \approx 2.5$ *according to* [2-5]

$\kappa_{\mathrm{P}} = \sqrt{8/\pi} \approx 1.6$ *according to* [6-7]

2. Evolution of the real contact area $A(p_0)$ for $\forall A/A_0$

$\frac{A}{A_0} = A(p_0, \alpha)/A_0$ *according to* [2-5]

$\frac{A}{A_0} = \mathrm{erf}\left(\sqrt{\frac{2}{\langle|\nabla h|^2\rangle}} \frac{p_0}{E^*}\right)$ *according to* [6-7]

[1] Greenwood, Williamson, P Roy Soc Lond A Mat 295 (1966)
[2] Bush, Gibson, Thomas, Wear 35 (1975)
[3] Mc Cool, Wear 107 (1986)
[4] Thomas, Rough Surfaces (1999)
[5] Greenwood, Wear 261 (2006)
[6] Persson, J. Chem. Phys. 115 (2001)
[7] Persson, Phys. Rev. Lett. 87 (2001)
[8] Persson, Bucher, Chiaia, Phys. Rev. B 65 (2002)
[9] Müser, Phys. Rev. Lett. 100, (2008)

Numerical methods: BEM vs FEM

Boundary Element Method (BEM)

- Rapid
- Periodic
- Elastic half-space
- Linear homogeneous elasticity

Finite Element Method (FEM)

- Slow
- Arbitrary boundary conditions
- Finite thickness
- Arbitrary non-linear / heterogeneous material

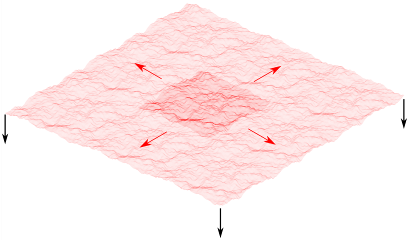

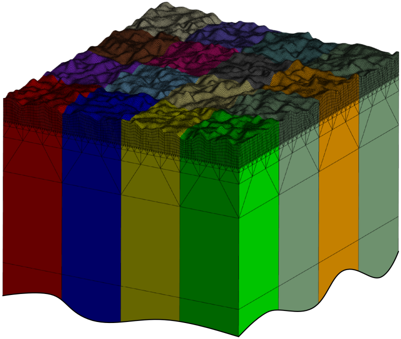

We use a parallel spectral based BEM

[1] Stanley & Kato, J Tribol 119 (1997)

FFT based BEM I

- Link between contact pressure and vertical displacement in full contact[1]

$$p(x,y) = \cos(2\pi k_x x/L)\cos(2\pi k_y y/L) \quad \Leftrightarrow$$

$$w(x,y) = \frac{2}{E^*\sqrt{k_x^2+k_y^2}}\cos(2\pi k_x x/L)\cos(2\pi k_y y/L)$$

$$w = \mathrm{FFT}^{-1}(K : \mathrm{FFT}(p))$$

- Optimization problem[2]

$$\min F = \int_A p[w/2+g]dA \quad \text{under conditions} \quad p \ge 0, \quad \int_A p dA = N$$

$$\min F = \sum f_{ij}[w_{ij}/2+g_{ij}], \quad f_{ij} \ge 0, \quad \sum f_{ij} = N$$

- Iterative procedure[1]

$$f^{k+1} = f^k - \nabla_p F^k, \quad \text{shift and truncate} \quad \tilde{f}_{ij}^{k+1} = \langle f_{ij}^{k+1} + \mathrm{const}\rangle, \quad \sum \tilde{f}_{ij}^{k+1} = N$$

[1] H.M. Stanley & T. Kato, An FFT-based method for Rough Surface Contact, J Tribol (1997)
[2] J.J. Kalker, Variational Principles of Contact Elastostatics, J Inst Maths Applics (1977)
See also [3] M. Paggi, A. Bemporad, Optimization algorithms for the solution of the frictionless normal contact between rough surfaces, Int J Solids Struct (2015)

FFT based BEM II

- **Convergence criteria**

Increment of functional: $|\Delta F/F| < \varepsilon_F$. Orthogonality: $\sum |f_{ij}g_{ij}|/N\bar{g}_0 < \varepsilon_O$

- **Consistent accuracy** $\varepsilon_D \sim \varepsilon_O$

$\tilde{f} = \langle f + \mathrm{const}\rangle$ such that $\sum \tilde{f} = N$. Solve by bisection: $|\sum \tilde{f} - N|/N < \varepsilon_D$

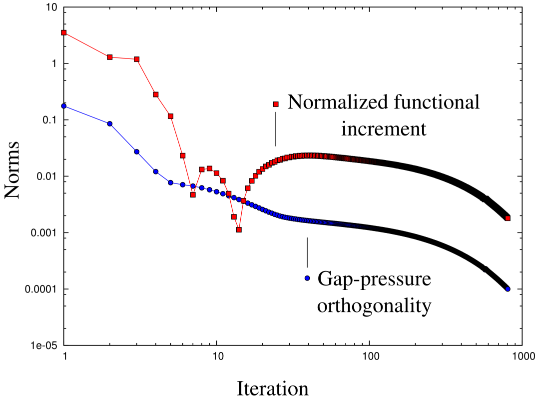

Example: $L \times L = 4096 \times 4096$, single CPU, only 5(!) minutes on laptop.

$L \times L = 1024 \times 1024$, 100 load increments, 50 surface realisations, $H = 0.8$

k_s=32 k_s=64 k_s=128

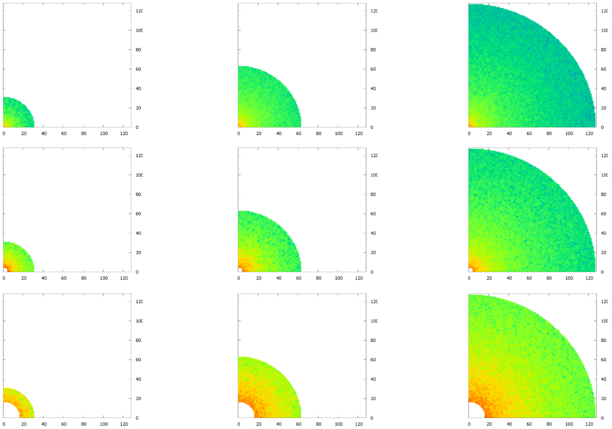

k_l=1

k_l=4

k_l=16

Surface PSD

Hu, Tonder. *Int. J. Mach. Tool Manuf.* 32 (1992)

Simulations

$L \times L = 1024 \times 1024$, 100 load increments, 50 surface realisations, $H = 0.8$

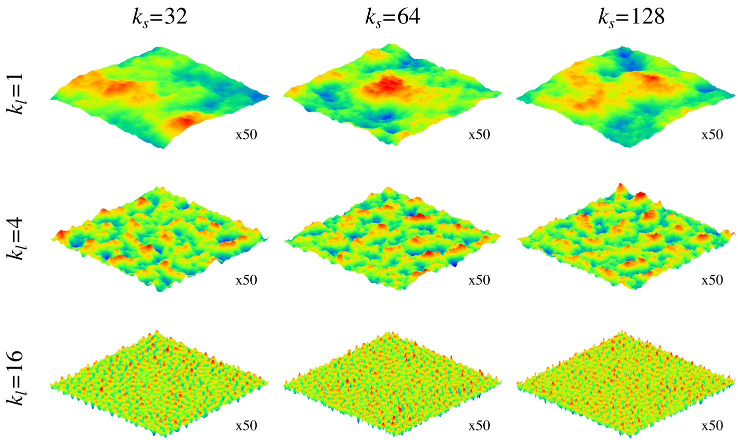

Surface roughness

Hu, Tonder. *Int. J. Mach. Tool Manuf.* 32 (1992)

Simulations

$L \times L = 1024 \times 1024$, 100 load increments, 50 surface realisations, $H = 0.8$

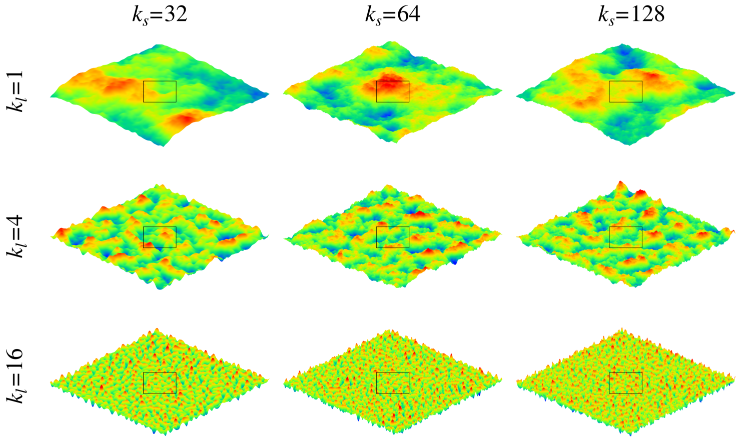

Surface roughness

Hu, Tonder. *Int. J. Mach. Tool Manuf.* 32 (1992)

Simulations

$L \times L = 1024 \times 1024$, 100 load increments, 50 surface realisations, $H = 0.8$

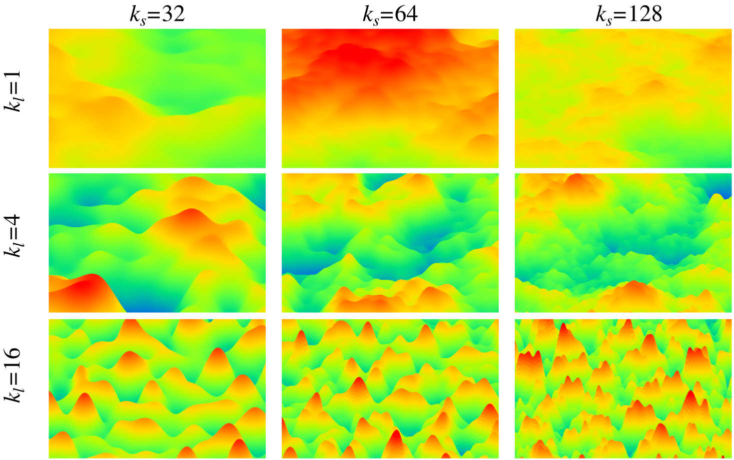

Surface roughness (zoom)

Hu, Tonder. *Int. J. Mach. Tool Manuf.* 32 (1992)

Real contact area evolution

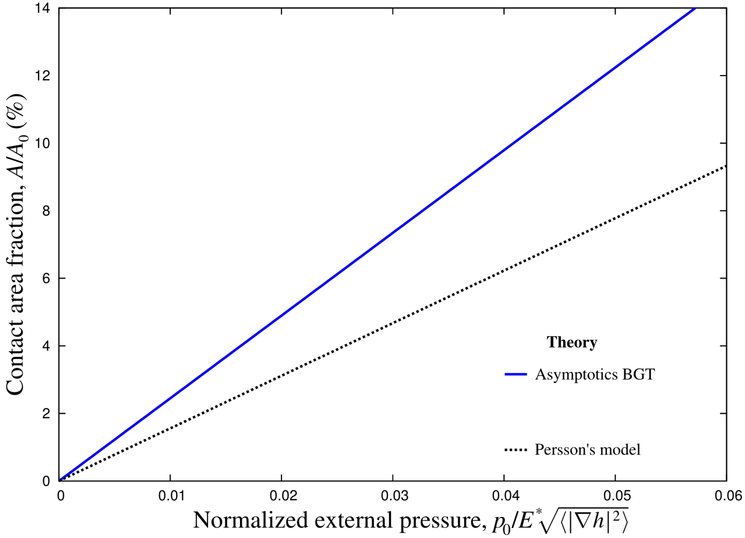

Real contact area evolution

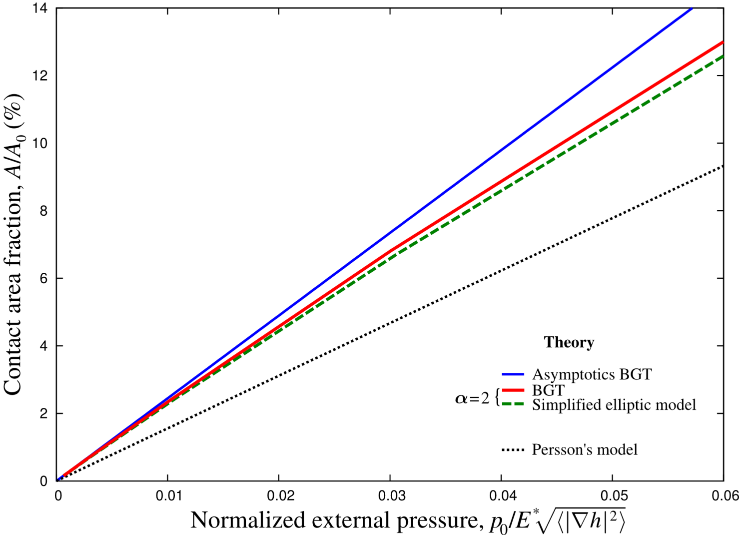

$\alpha = 2,\ 10$ from[1]

[1] Carbone, Bottiglione, J. Mech. Phys. Solids 56 (2008).

Real contact area evolution

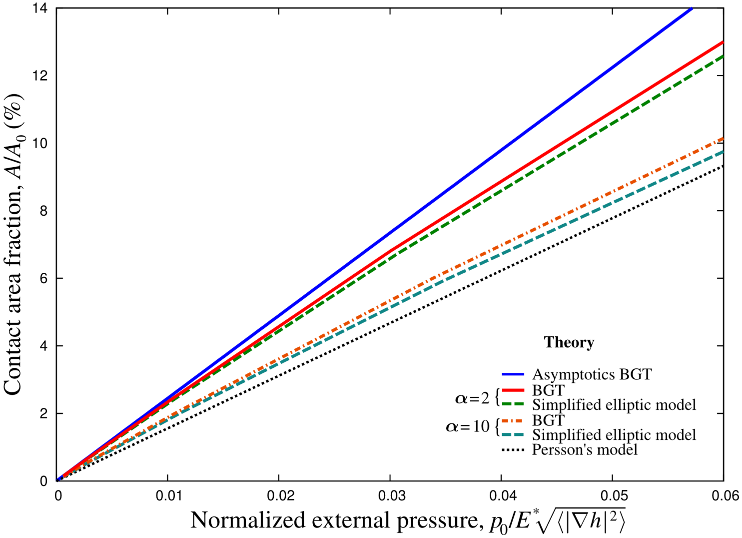

$\alpha = 2,\ 10$ from[1]

[1] Carbone, Bottiglione, J. Mech. Phys. Solids 56 (2008).

Real contact area evolution

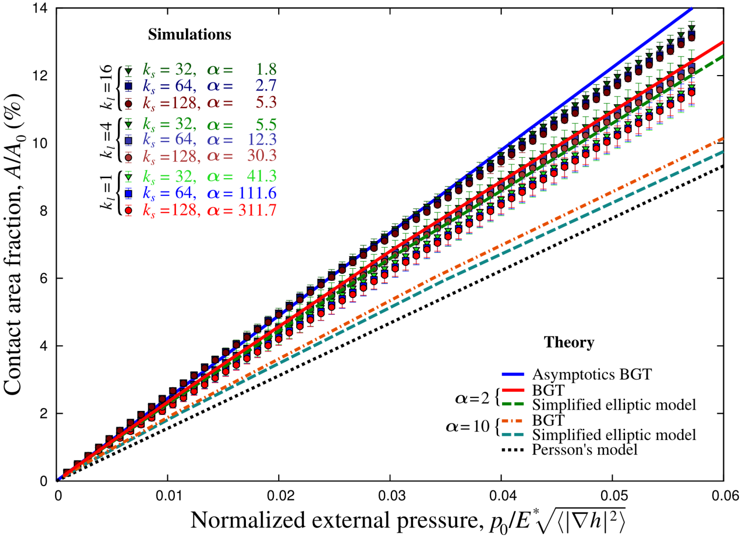

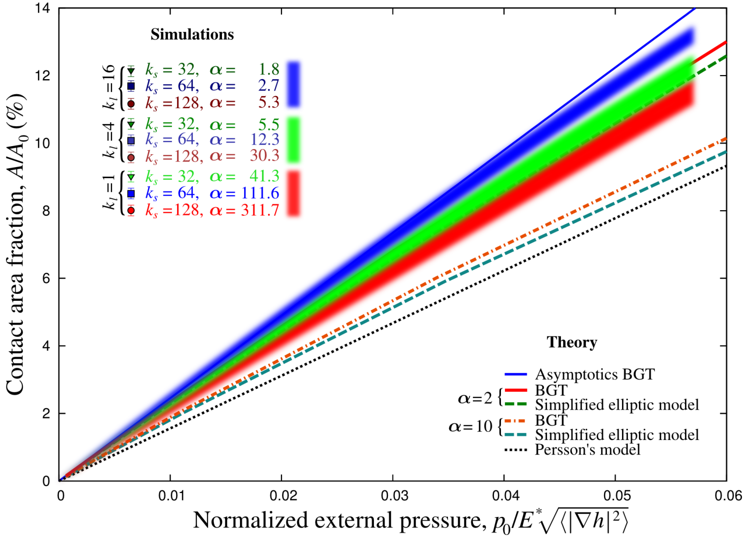
Simulations
$k_l=16$: $k_s = 32$, $\alpha = 1.8$; $k_s = 64$, $\alpha = 2.7$; $k_s = 128$, $\alpha = 5.3$
$k_l=4$: $k_s = 32$, $\alpha = 5.5$; $k_s = 64$, $\alpha = 12.3$; $k_s = 128$, $\alpha = 30.3$
$k_l=1$: $k_s = 32$, $\alpha = 41.3$; $k_s = 64$, $\alpha = 111.6$; $k_s = 128$, $\alpha = 311.7$
Theory
Asymptotics BGT
$\alpha=2$: BGT, Simplified elliptic model
$\alpha=10$: BGT, Simplified elliptic model
Persson's model
Contact area fraction, A/A_0 (%)
Normalized external pressure, $p_0/E^*\sqrt{\langle|\nabla h|^2\rangle}$
0
2
4
6
8
10
12
14
0
0.01
0.02
0.03
0.04
0.05
0.06

- **Conclusions I:**
  - Effect of α is overestimated in analytical models without interaction *(confirmed older results[1])*
  - Representative surfaces (high k_l) yield higher contact area and less dispersion *(yet no convergence is found)*

[1] Paggi, Ciavarella. *Wear* 268 (2010)

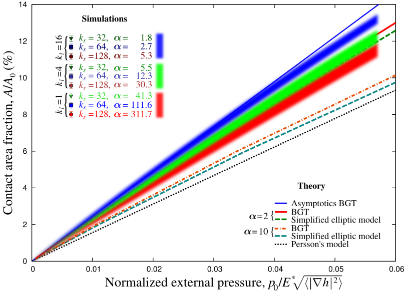

Fig. Contact area evolution

Real contact area evolution

- **Conclusions I:**
  - Effect of α is overestimated in analytical models without interaction
    (confirmed older results[1])
  - Representative surfaces (high k_l) yield higher contact area and less dispersion
    (yet no convergence is found)

[1] Paggi, Ciavarella. *Wear* 268 (2010)

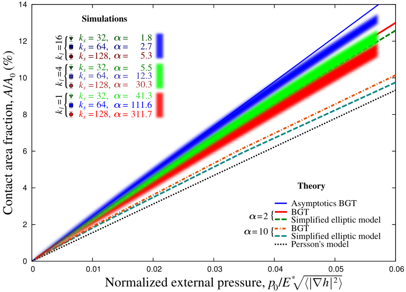

Fig. Contact area evolution

- What about the proportionality coefficient κ?

How to estimate κ?

$$\frac{A}{A_0} = \frac{\kappa}{\sqrt{\langle|\nabla h|^2\rangle}}\frac{p_0}{E^*}$$

$$A = A(p_0)$$

$$\boxed{\kappa = \sqrt{\langle|\nabla h|^2\rangle}\,E^*\left\{\lim_{p_0\to 0}\frac{\partial A/A_0}{\partial p_0}\right\}}$$

Instead, in the literature, the secant is often used at given separation[1] d/σ or at given pressure[2] p_0, *viz.* $\kappa_s(*) = E^*\sqrt{\langle|\nabla h|^2\rangle}\frac{A}{p_0 A_0}$

[1] Paggi, Ciavarella. *Wear* 268 (2010)
[2] Prodanov, Dapp, Müser. *Tribol. Lett.* 53 (2014)

Simulations[1-3] predict that κ depends on the Hurst exponent H, except[4]

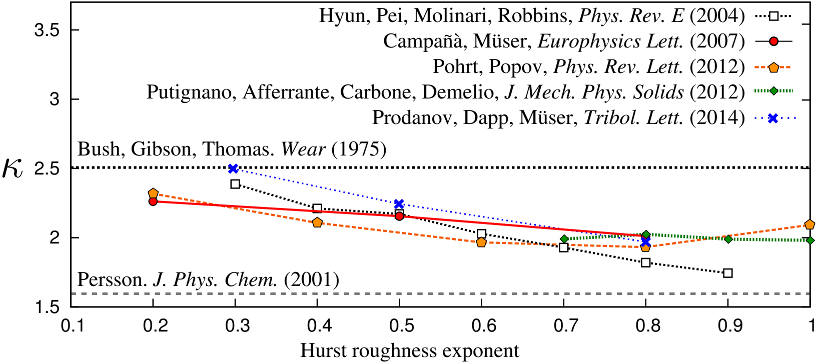

All simulations are carried out for non-representative surfaces $k_l = 1$, except[5]

[1] Hyun, Pei, Molinari, Robbins. *Phys. Rev. E* 70 (2004)
[2] Campañà, Müser. *Europhys. Lett.* 77 (2007)
[3] Pohrt, Popov. *Phys. Rev. Lett.* 108 (2012)
[4] Putignano, Afferrante, Carbone, Demelio. *J. Mech. Phys. Solids* 60 (2012)

⋆[5] Prodanov, Dapp, Müser. *Tribol. Lett.* 53 (2014)

Simulations[1-3] predict that κ depends on the Hurst exponent H, except[4]

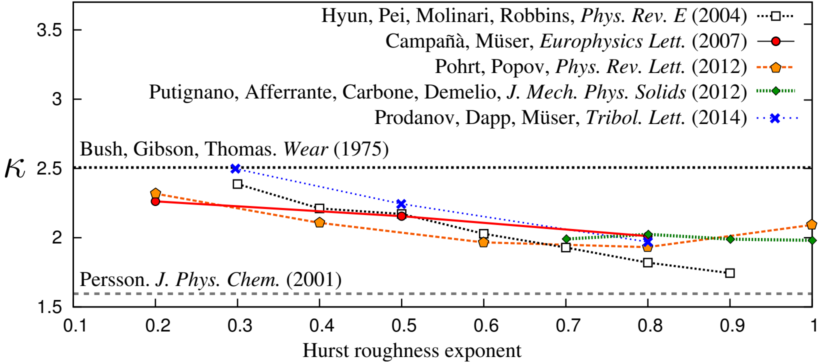

All simulations are carried out for non-representative surfaces $k_l = 1$, except[5]

[1] Hyun, Pei, Molinari, Robbins. *Phys. Rev. E* 70 (2004)
[2] Campañà, Müser. *Europhys. Lett.* 77 (2007)
[3] Pohrt, Popov. *Phys. Rev. Lett.* 108 (2012)
[4] Putignano, Afferrante, Carbone, Demelio. *J. Mech. Phys. Solids* 60 (2012)

⋆[5] Prodanov, Dapp, Müser. *Tribol. Lett.* 53 (2014)

⋆⋆[6] Paggi, Ciavarella. *Wear* 268 (2010)

The state of the art: simulations

A more rich result with asperity-based and complete models

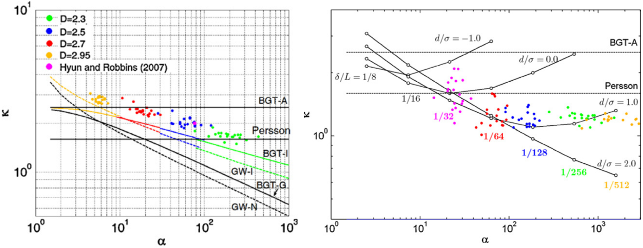

Fig. Secant-defined κ evolution[6] with respect to Nayak parameter α

[6] Paggi, Ciavarella. *Wear* 268 (2010)

A more rich result with asperity-based and complete models

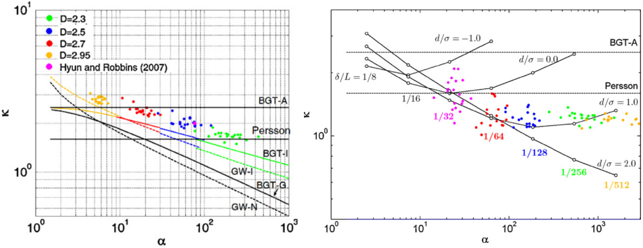

Fig. Secant-defined κ evolution[6] with respect to Nayak parameter α

A link[7,8] between Hurst exponent H, Nayak parameter α and magnification $\zeta = k_s/k_l$

$$\alpha(H,\zeta) = \frac{3}{2}\,\frac{(1-H)^2}{H(H-2)}\,\frac{(\zeta^{-2H}-1)(\zeta^{4-2H}-1)}{(\zeta^{2-2H}-1)^2},$$

[6] Paggi, Ciavarella. *Wear* 268 (2010)
[7] Bottiglione, Carbone, Mantriota. *Tribol. Int.* 42 (2009)
[8] Yastrebov, Anciaux, Molinari, *Int. J. Solids Struct.* 52 (2015)

The state of the art: simulations

Simulations[1-3] predict that κ depends on the Hurst exponent H, except[4]

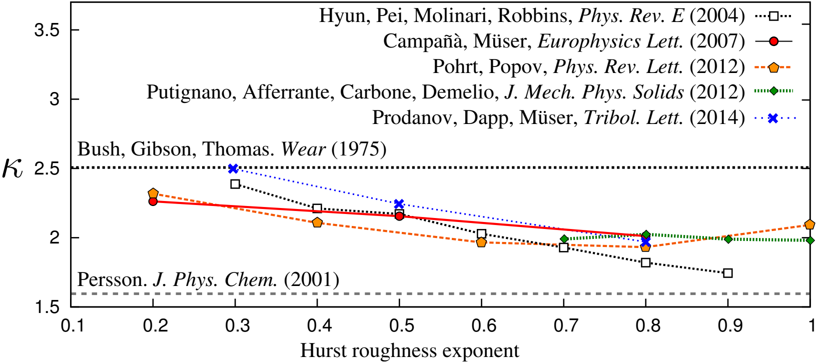

All simulations are carried out for non-representative surfaces $k_l = 1$, except[5]

[1] Hyun, Pei, Molinari, Robbins. *Phys. Rev. E* 70 (2004)
[2] Campañà, Müser. *Europhys. Lett.* 77 (2007)
[3] Pohrt, Popov. *Phys. Rev. Lett.* 108 (2012)
[4] Putignano, Afferrante, Carbone, Demelio. *J. Mech. Phys. Solids* 60 (2012)

★[5] Prodanov, Dapp, Müser. *Tribol. Lett.* 53 (2014)

★★[6] Paggi, Ciavarella. *Wear* 268 (2010)

Results

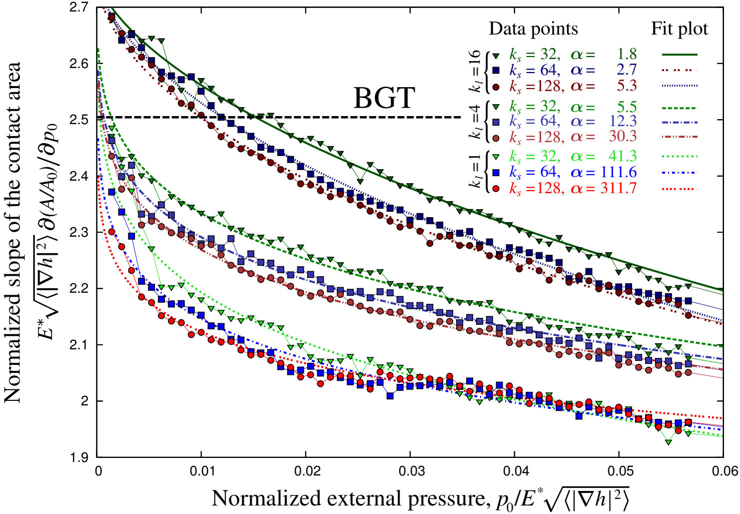

Fig. Contact area slope evolution

BGT: Bush, Gibson, Thomas, Wear 35 (1975)

Results

- **Conclusions II:**
  - Linearity between the contact area and the pressure is not observed
  - The coefficient κ is hard to evaluate
  - Need to go for a more complete description of the contact area evolution

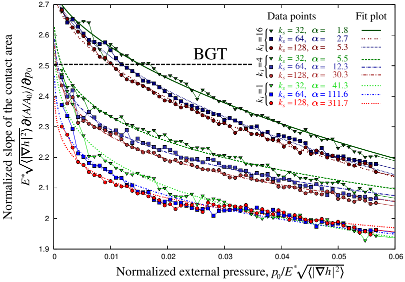

Fig. Contact area slope evolution

- **Conclusions II:**
  - Linearity between the contact area and the pressure is not observed
  - The coefficient κ is hard to evaluate
  - Need to go for a more complete description of the contact area evolution

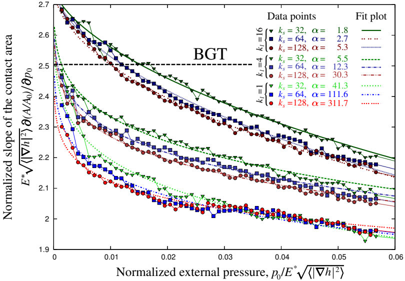

Fig. Contact area slope evolution

- **What can we deduce from it?**

A phenomenological equation for the contact area evolution[1,2]:

$$A/A_0 = \left[\beta + \left(\frac{E^*\sqrt{\langle|\nabla h|^2\rangle}}{\kappa p_0}\right)^{\mu}\right]^{-1/\mu} \xrightarrow[p_0\to 0]{} \frac{\kappa p_0}{E^*\sqrt{\langle|\nabla h|^2\rangle}}$$

[1] Yastrebov, Anciaux, Molinari, Phys. Rev. E 86 (2012)
[2] Yastrebov, Anciaux, Molinari, Int. J. Solids Struct. 52 (2015)

Contact area up to full contact

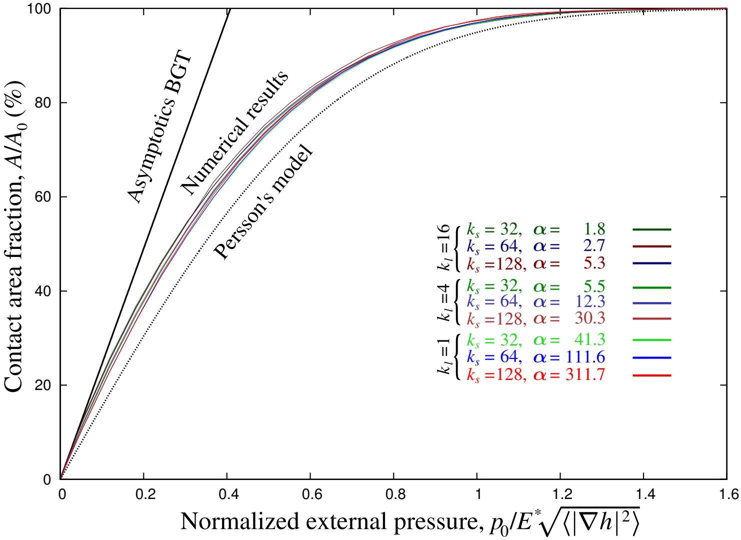

Fig. Area evolution up to full contact

Real contact area morphology

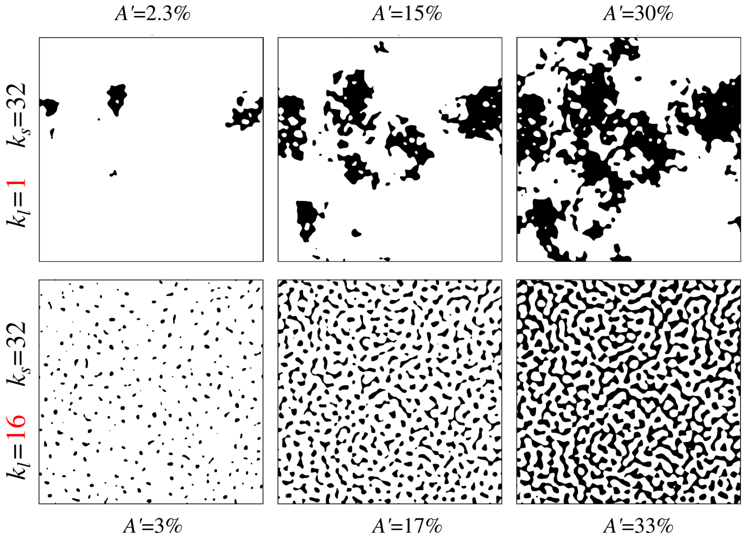

[1] Yastrebov, Anciaux, Molinari, Int. J. Solids Struct. 52 (2015)

Real contact area morphology

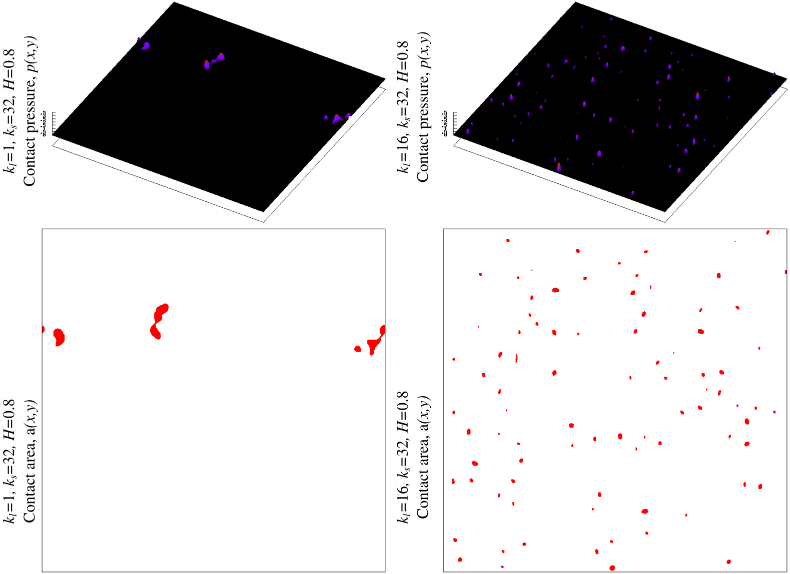

[1] Yastrebov, Anciaux, Molinari, Int. J. Solids Struct. 52 (2015)

Objective

- Contact static seal
- Numerical analysis of leakage between rough surfaces in contact
- Effect of roughness and material on sealing properties

• Fluid analysis

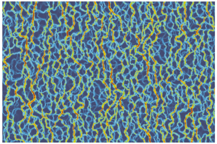

• Roughness analysis

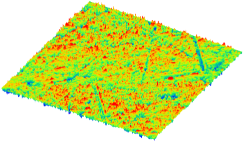

Fractal dimension / rms gradient
spectrum breadth

• Mechanical contact analysis

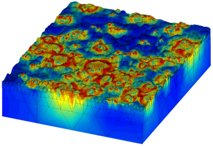

Elastic / visco-elastic
visco-plastic / crystal plasticity

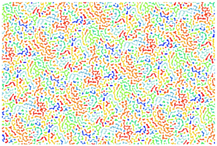

• Percolation analysis

Applications:

- Seals, gaskets, etc.
- Hydraulic fracturing
- Gas extraction from cracked rocks

- 3D FE mesh of residual volume + full 3D CFD analysis

OR

- 2D Reynolds equation for viscous Poiseuille flow

$$\nabla \cdot (h^3(x,y)\nabla p) = 0, \qquad q = \frac{h^3(x,y)}{12\mu}\nabla p$$

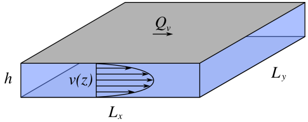

- Transmissivity

$$K = Q_v \frac{L_x}{L_y}\frac{\mu}{\Delta p}$$

3D CFD (Abaqus)
*Viscous flow (**Z-set**, in-house FE software)*

Z-set Material & structure analysis suite

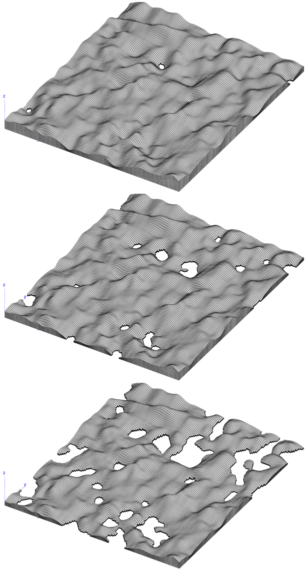

[1] J. Durand, PhD Thesis (2012)

- 3D FE mesh of residual volume + full 3D CFD analysis

OR

- 2D Reynolds equation for viscous Poiseuille flow

$$\nabla \cdot (h^3(x,y)\nabla p) = 0, \quad q = \frac{h^3(x,y)}{12\mu}\nabla p$$

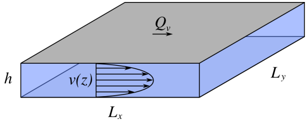

- Transmissivity

$$K = Q_v \frac{L_x}{L_y}\frac{\mu}{\Delta p}$$

3D CFD (Abaqus)
*Viscous flow (**Z-set**, in-house FE software)*

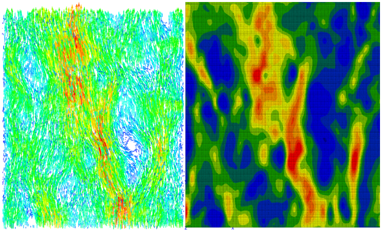

Fig. 3D CFD and Reynolds simulations (flow rate)

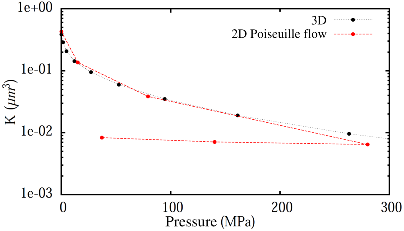

Fig. Comparison 3D CFD vs Reynolds simulation (transmissivity)

[1] J. Durand, PhD Thesis (2012)

Fluid flow through contact interface

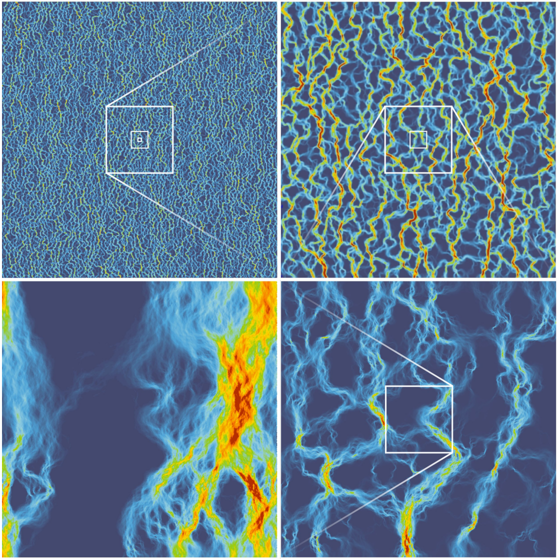

Fig. Fluid flow for rough surfaces with $k_l = 64 > 16 > 4 > 1$,
i.e. for system sizes $L \times L = 4096 > 256 > 16 > 1$.

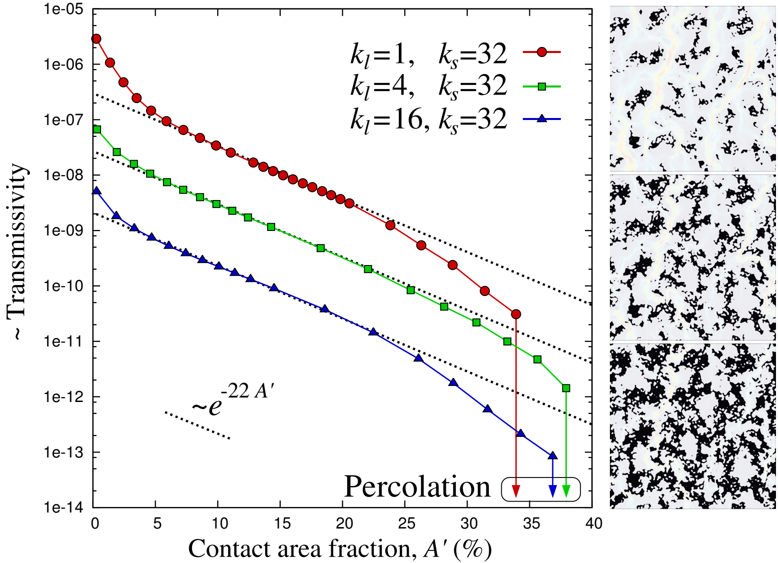

Fig. Transmissivity evolution with increasing contact area

Mechanical (BEM) and fluid (FEM) simulations with mesh $N \times N = 2048 \times 2048$

Four phases:

- I Transitional 1
- II Stationary
- III Transitional 2 – *Percolation*
- IV No-leakage

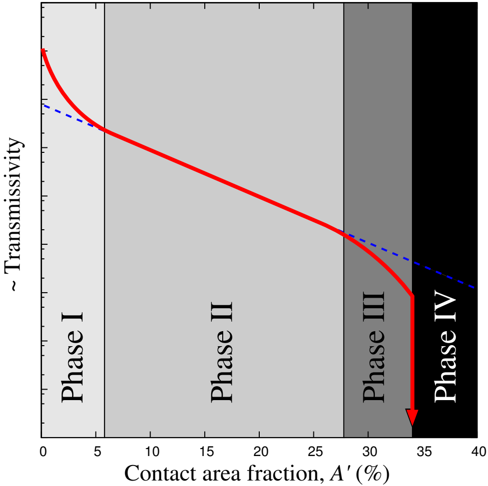

Based on simulations on mesh $L \times L = 2048 \times 2048$ for all combinations of $k_l = 1, 4, 16 \times k_s = 32, 64, 128 \times H = 0.3, 0.5, 0.8 \times 5$ realizations, **1.9 Tb(!)** of data

Fluid flow through contact interface

Four phases:

I Transitional 1

reduces if Gaussianity increases ($k_l \gg 1$)

II Stationary

exponential decrease

$K \sim \exp(-\gamma A')$

$\gamma \approx 22 - 25$

III Transitional 2 – *Percolation*

at $A'_{perc} \approx 35 - 40\%$ [1,2,3]

IV No-leakage

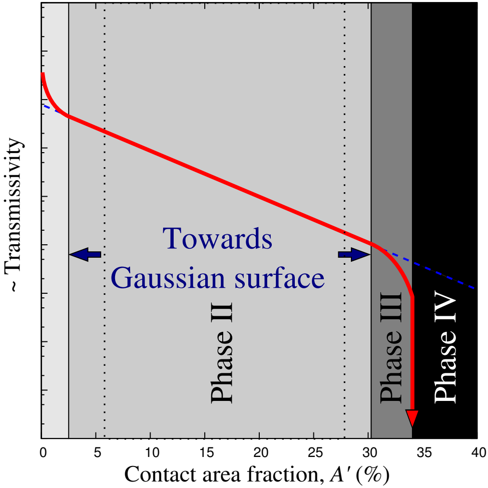

$A'_{perc} \approx 40.0\%$ [1] Stauffer, Aharony, Introduction to percolation theory (2003)

$A'_{perc} \approx 42.5\%$ [2] Dapp, Lücke, Persson, Müser, *Phys. Rev. Lett.* 108 (2012)

$A'_{perc} \approx 35.4\%$ [3] Putignano, Afferante, Carbone, Demelio. *Tribol. Int.* 64 (2013).

Based on simulations on mesh $L \times L = 2048 \times 2048$ for all combinations of $k_l = 1, 4, 16 \times k_s = 32, 64, 128 \times H = 0.3, 0.5, 0.8 \times 5$ realizations, **1.9 Tb(!)** of data

Phenomenological model for sealing

- **Transmissivity**

$$K \sim \frac{Q}{\Delta P}$$

- **Flow rate** with respect to contact area fraction

$$Q \sim \langle h^2 \rangle^{3/2} \exp(-\gamma A'), \quad \gamma \approx 22 - 25$$

- **Contact area** evolution with pressure (up to 35%)[1]

$$A' = \left[\beta + \left(\frac{E^* \sqrt{\langle|\nabla h|^2\rangle}}{\kappa p_0}\right)^{\mu}\right]^{-1/\mu} \xrightarrow[p_0 \to 0]{} \frac{\kappa p_0^{[2]}}{E^* \sqrt{\langle|\nabla h|^2\rangle}}$$

$A' = A/A_0$ *relative contact area,* E^* *effective elastic modulus,* p_0 *external pressure,* $\sqrt{\langle|\nabla h|^2\rangle}$ *rms slope and* $\beta \approx 0.21, \mu \approx 0.45, \kappa \approx \sqrt{2\pi}$ *are three constants.*

- For stationary regime:

$$K \sim \frac{\langle h^2 \rangle^{3/2}}{\Delta P} \exp\left(-\gamma \left[\beta + \left(\frac{E^* \sqrt{\langle|\nabla h|^2\rangle}}{\kappa p_0}\right)^{\mu}\right]^{-1/\mu}\right)$$

[1] Yastrebov, Anciaux, Molinari, *Phys. Rev. E* 86 (2012)
[2] Bush, Gibson, Thomas, *Wear* 35 (1975)

Towards the percolation limit

- Not accurate detection of the percolation limit in fluid simulations
- Need a cluster analysis
- Critical junction approach
- Percolation limit[1,2,3]

  $A'_{\mathrm{perc}} \approx 35 - 40\%$

  in contrast to the overlap model

  $A'_{\mathrm{overlap}} = 50\%$

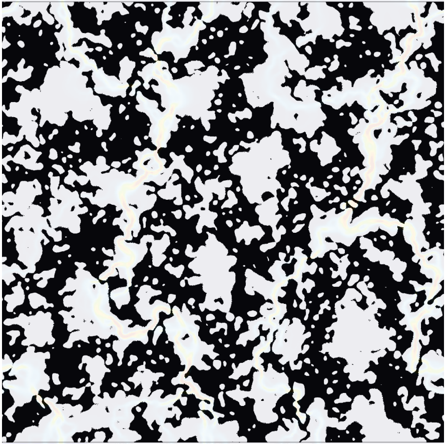

Fig. Percolation through non-percolating cluster

$A'_{\mathrm{perc}} \approx 40.0\%$ [1] Stauffer, Aharony, Introduction to percolation theory (2003)

$A'_{\mathrm{perc}} \approx 42.5\%$ [2] Dapp, Lücke, Persson, Müser, *Phys. Rev. Lett.* 108 (2012)

$A'_{\mathrm{perc}} \approx 35.4\%$ [3] Putignano, Afferante, Carbone, Demelio. *Tribol. Int.* 64 (2013).

Towards the percolation limit

- Not accurate detection of the percolation limit in fluid simulations
- Need a cluster analysis
- Critical junction approach
- Percolation limit[1,2,3]

  $A'_{\text{perc}} \approx 35 - 40\%$

  in contrast to the overlap model

  $A'_{\text{overlap}} = 50\%$

$A'_{\text{perc}} \approx 40.0\%$ [1] Stauffer, Aharony, Introduction to percolation theory (2003)
$A'_{\text{perc}} \approx 42.5\%$ [2] Dapp, Lücke, Persson, Müser, *Phys. Rev. Lett.* 108 (2012)
$A'_{\text{perc}} \approx 35.4\%$ [3] Putignano, Afferante, Carbone, Demelio. *Tribol. Int.* 64 (2013).

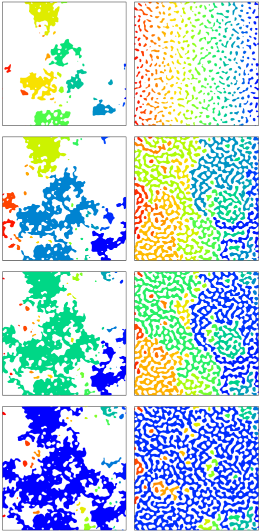

Fig. Detection of contact clusters and search for an infinite cluster

- Not accurate detection of the percolation limit in fluid simulations
- Need a cluster analysis
- Critical junction approach
- Percolation limit[1,2,3]

  $A'_{\text{perc}} \approx 35 - 40\%$

  in contrast to the overlap model

  $A'_{\text{overlap}} = 50\%$
- Back to discrete percolation[4,5]

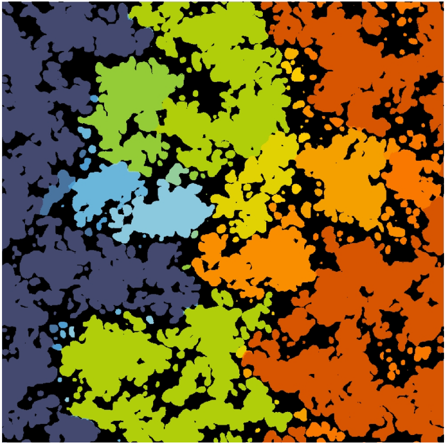

Fig. Hydrostatic pressure cells, contact zones (black) and fluid flux

[4] Isichenko, Rev. Mod. Phys. 64 (1992)
[5] Stauffer, Aharony, Introduction to percolation theory (2003)

Towards the percolation limit

- Not accurate detection of the percolation limit in fluid simulations
- Need a cluster analysis
- Critical junction approach
- Percolation limit[1,2,3]

  $A'_{\text{perc}} \approx 35-40\%$

  in contrast to the overlap model

  $A'_{\text{overlap}} = 50\%$
- Back to discrete percolation[4,5]

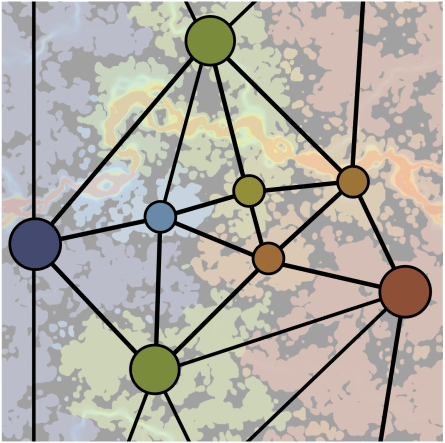

Fig. A graph connecting hydrostatic pressure cells

[4] Isichenko, Rev. Mod. Phys. 64 (1992)
[5] Stauffer, Aharony, Introduction to percolation theory (2003)

Conclusions III

- Take care of surface representativity $k_l \gg 1$, i.e. $\lambda_l \ll L$.
- Different regimes of leakage
- For stationary regime

$$Q \sim \langle h^2 \rangle^{3/2} \exp(-\gamma A'), \quad \gamma \approx 22 - 25,$$

Q - flow rate, A' - contact area fraction.

- Transmissivity (K) evolution with pressure (p_0)

$$K \sim \frac{\langle h^2 \rangle^{3/2}}{\Delta P} \exp\left(-\gamma \left[\beta + \left(\frac{E^* \sqrt{\langle |\nabla h|^2 \rangle}}{\kappa p_0}\right)^{\mu}\right]^{-1/\mu}\right)$$

ΔP - fluid pressure drop, E^* - effective elastic modulus, $\sqrt{\langle |\nabla h|^2 \rangle}$ - rms slope.

- Percolation limit

$$\boxed{A'_{\text{perc}} \approx 35 - 40\%} \quad < \quad 50\% = A'_{\text{overlap}}$$

- From continuum percolation to percolation on lattice

Towards strong coupling I

- **Weak coupling:** solve solid → solve fluid
- **Strong coupling:** solve solid **AND** fluid
  - ⋆ Iterative scheme:
  - solve solid → solve fluid → solid → fluid → . . .
  - Data exchange:
  - solid → fluid: gap $g(x,y)$
  - fluid → solid: hydrostatic pressure $p(x,y)$

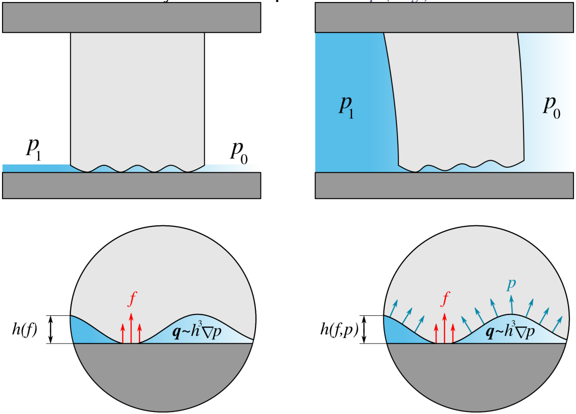

- **Exponential convergence**

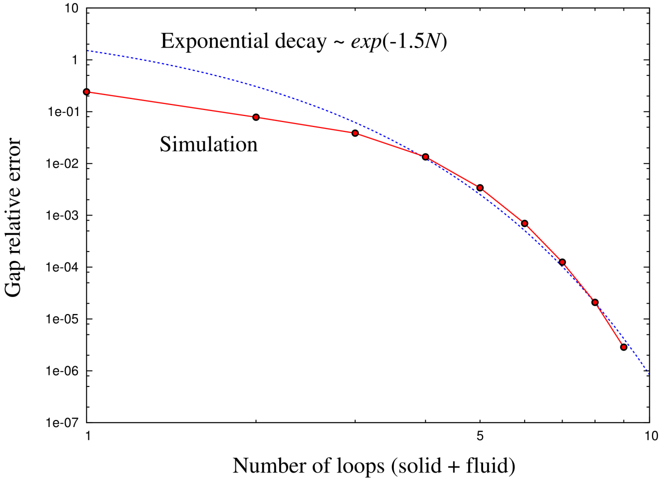

Towards strong coupling II

- **Exponential convergence**
- **Issues**
  - Trapped incompressible fluid $V^i = \int_{A_t^i} g(x,y)\,dA = \mathrm{const}$
  - Coupling beyond percolation limit $\nabla p = 0$

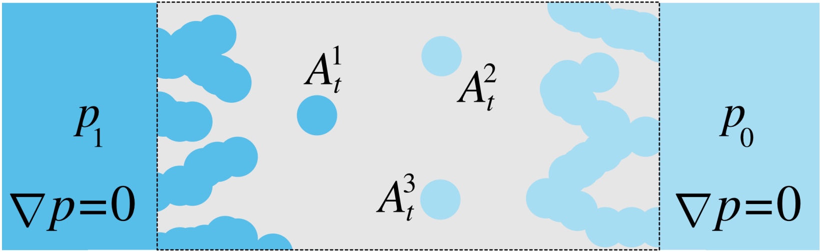

Strong coupling: example

- Hydrostatic pressure drop 500 bar (50 MPa)
- Young's modulus 2 GPa
- Characteristic size 1 cm

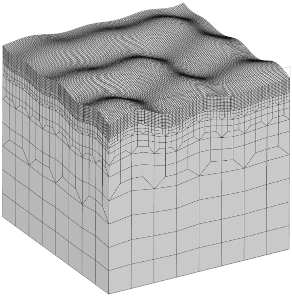

Strong coupling: example

- Hydrostatic pressure drop 500 bar (50 MPa)
- Young's modulus 2 GPa
- Characteristic size 1 cm

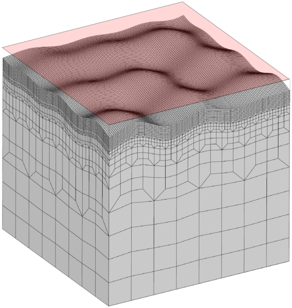

Strong coupling: example

- Hydrostatic pressure drop 500 bar (50 MPa)
- Young's modulus 2 GPa
- Characteristic size 1 cm

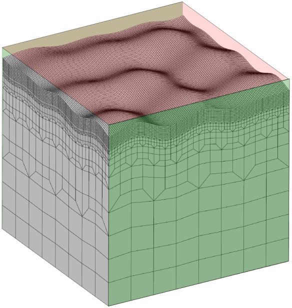

Strong coupling: example

- Hydrostatic pressure drop 500 bar (50 MPa)
- Young's modulus 2 GPa
- Characteristic size 1 cm

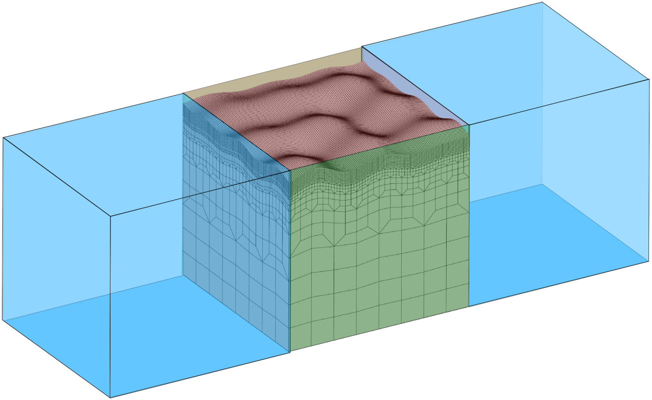

Strong coupling: example

- Hydrostatic pressure drop 500 bar (50 MPa)
- Young's modulus 2 GPa
- Characteristic size 1 cm

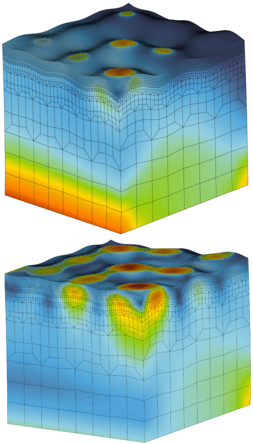

von Mises stress

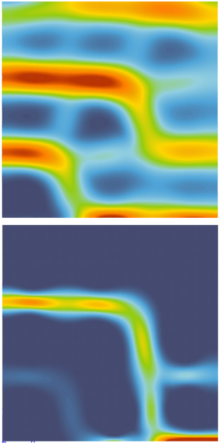

$|\nabla \boldsymbol{q}|$

Strong coupling: example

- Hydrostatic pressure drop 500 bar (50 MPa)
- Young's modulus 2 GPa
- Characteristic size 1 cm

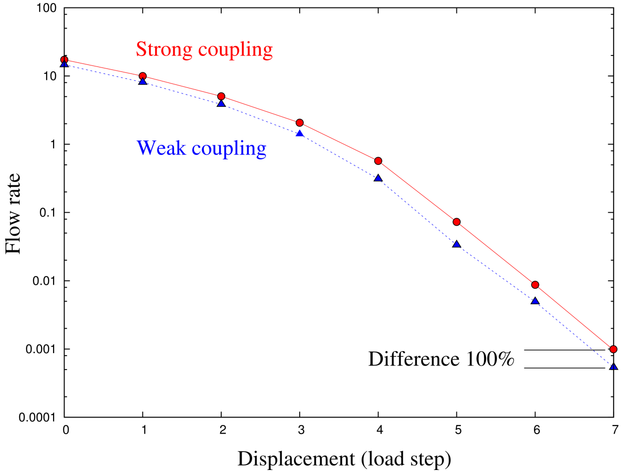

Conclusion

- Mechanical contact is critical for sealing problem
- Representativity $\Leftrightarrow$ $k_l > 4$
- Weak coupling: complete analysis

- Iterative strong coupling scheme works well
- Strong coupling may be important
- But the effect of trapped fluid should be more critical

Conclusion

- Mechanical contact is critical for sealing problem
- Representativity $\Leftrightarrow$ $k_l > 4$
- Weak coupling: complete analysis

- Iterative strong coupling scheme works well
- Strong coupling may be important
- But the effect of trapped fluid should be more critical

Thank you for your attention!

<vladislav.yastrebov@mines-paristech.fr> www.yastrebov.fr

- Lattice models[1,2]
- Average separation analysis for ***stationary regime***
  use asperity-based or Persson models[3,4]
- Critical constriction or critical junction approach for ***near percolation regime***[4,5]
- Complete analysis[6]

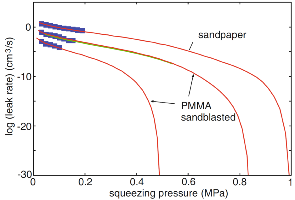

Fig. Flow rate w.r.t. contact pressure[4]

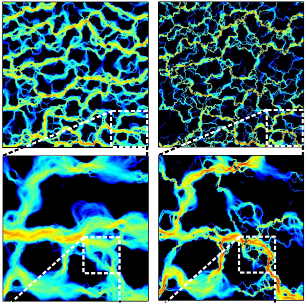

Fig. Flow density overlap VS elastic models[6]

[1] Plouraboué, Geoffroy, Prat. *Phys. Fluids* 16 (2004)

[2] Flukiger, Plouraboué, Prat. *Phys. Rev. E* 77 (2008)

[3] Bottiglione, Carbone, Mantriota. *Tribol. Int.* 42 (2009)

[4] Lorenz, Persson. *Eur. Phys. J. E* 31 (2010)

[5] Dapp, Müser. *Europhys. Lett.* 109 (2015)

[6] Dapp, Lücke, Persson, Müser. *Phys. Rev. Lett.* 108 (2012)

Mechanical contact VS overlap model

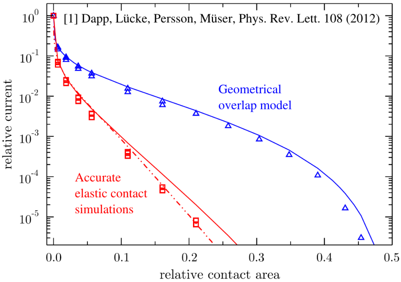

Fig. Comparison of leakage between a mechanical contact model and a geometrical overlap model[1]

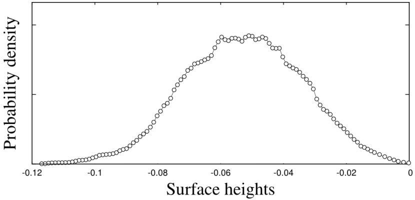

Fig. Original PDF of heights

[1] Dapp, Lücke, Persson, Müser, *Phys. Rev. Lett.* 108 (2012)

Mechanical contact VS overlap model

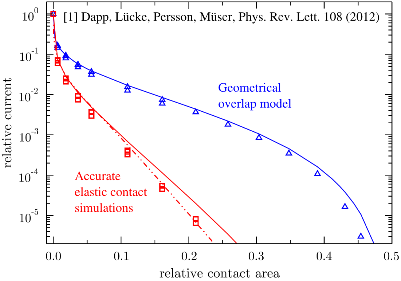

Fig. Comparison of leakage between a mechanical contact model and a geometrical overlap model[1]

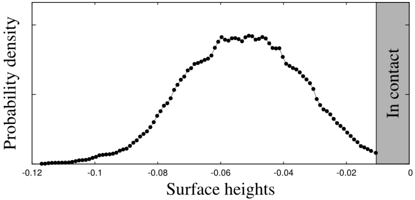

Fig. Overlap model: PDF at $A' \approx 0.3\%$

[1] Dapp, Lücke, Persson, Müser, *Phys. Rev. Lett.* 108 (2012)

Mechanical contact VS overlap model

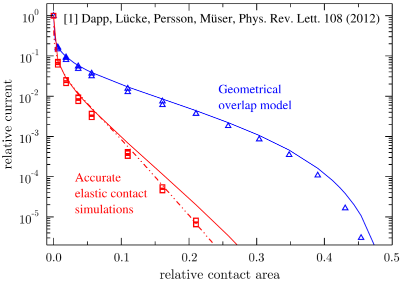

Fig. Comparison of leakage between a mechanical contact model and a geometrical overlap model[1]

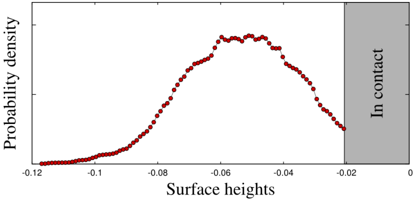

Fig. Overlap model: PDF at $A' \approx 1.9\%$

[1] Dapp, Lücke, Persson, Müser, *Phys. Rev. Lett.* 108 (2012)

Mechanical contact VS overlap model

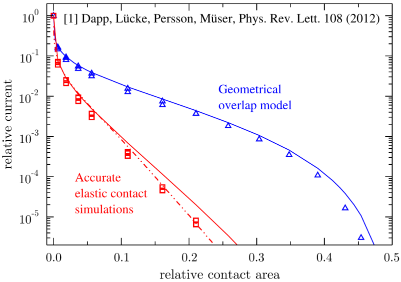

Fig. Comparison of leakage between a mechanical contact model and a geometrical overlap model[1]

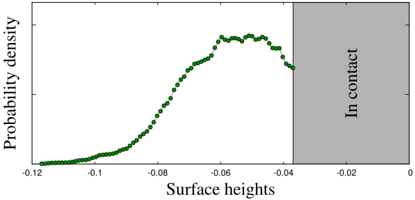

Fig. Overlap model: PDF at A′ ≈ 10%

[1] Dapp, Lücke, Persson, Müser, *Phys. Rev. Lett.* 108 (2012)

Mechanical contact VS overlap model

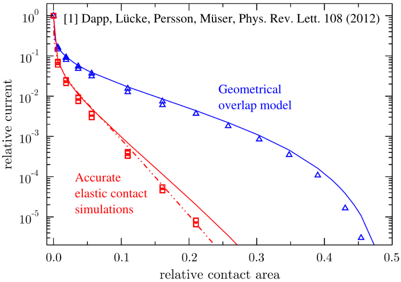

Fig. Comparison of leakage between a mechanical contact model and a geometrical overlap model[1]

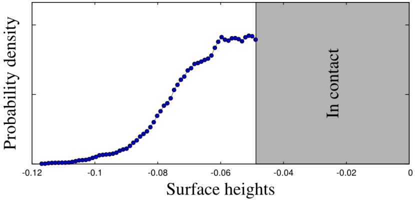

Fig. Overlap model: PDF at $A' \approx 22\%$

[1] Dapp, Lücke, Persson, Müser, *Phys. Rev. Lett.* 108 (2012)

Mechanical contact VS overlap model

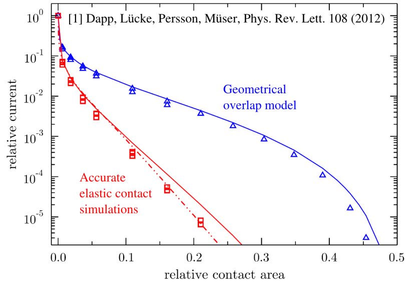

Fig. Comparison of leakage between a mechanical contact model and a geometrical overlap model[1]

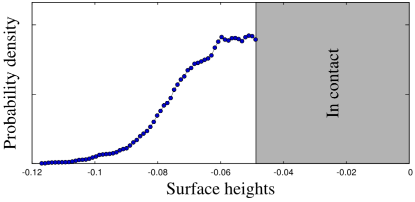

Fig. Overlap model: PDF at $A' \approx 22\%$

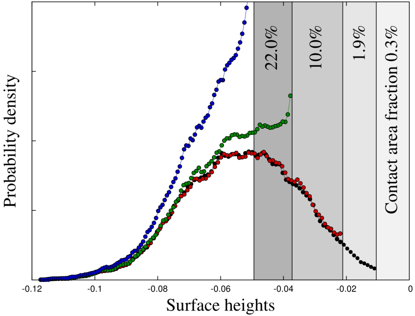

Fig. Mechanical contact

[1] Dapp, Lücke, Persson, Müser, *Phys. Rev. Lett.* 108 (2012)

- Contact of elastic regular wavy surface[1] (revisited[2,3])

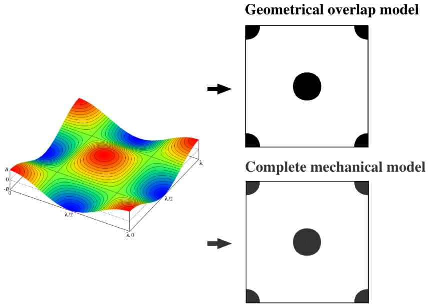

Contact clusters in mechanical contact tend to coalesce

[1] Johnson, Greenwood, Higginson, *Int. J. Mech. Sci.* 27 (1985)
[2] Yastrebov, Anciaux, Molinari, *Tribol. Lett.* 56 (2014)
[3] Dapp, Müser, *Europhys. Lett.* 109 (2015)

- Contact of elastic regular wavy surface[1] (revisited[2,3])

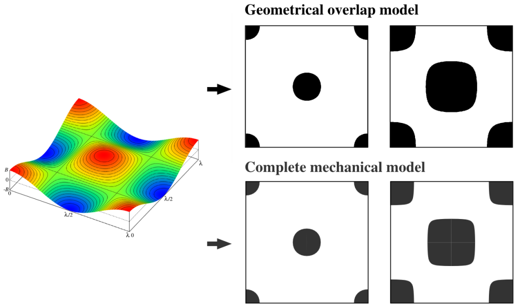

Contact clusters in mechanical contact tend to coalesce

[1] Johnson, Greenwood, Higginson, *Int. J. Mech. Sci.* 27 (1985)
[2] Yastrebov, Anciaux, Molinari, *Tribol. Lett.* 56 (2014)
[3] Dapp, Müser, *Europhys. Lett.* 109 (2015)

- Contact of elastic regular wavy surface[1] (revisited[2,3])

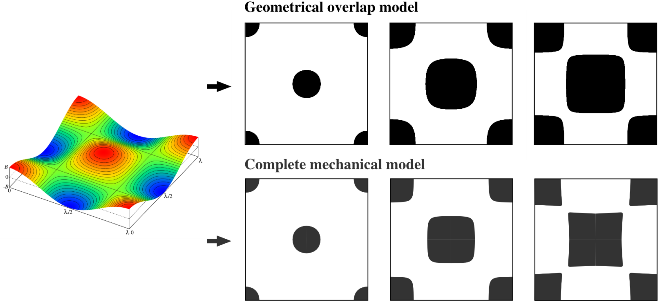

Contact clusters in mechanical contact tend to coalesce

[1] Johnson, Greenwood, Higginson, *Int. J. Mech. Sci.* 27 (1985)
[2] Yastrebov, Anciaux, Molinari, *Tribol. Lett.* 56 (2014)
[3] Dapp, Müser, *Europhys. Lett.* 109 (2015)

Mechanical contact VS overlap model

- Contact of elastic regular wavy surface[1] (revisited[2,3])

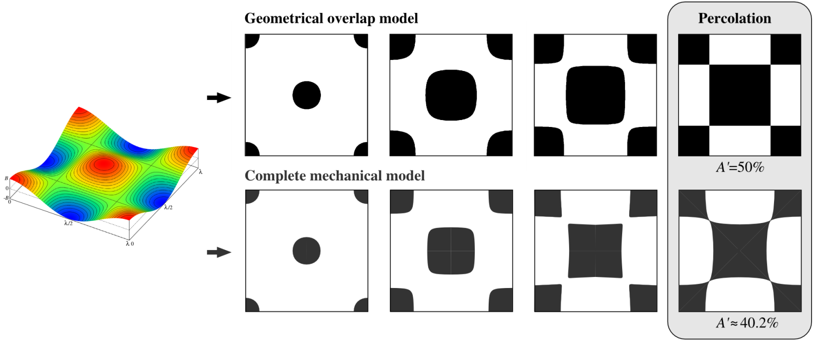

Contact clusters in mechanical contact tend to coalesce

[1] Johnson, Greenwood, Higginson, *Int. J. Mech. Sci.* 27 (1985)
[2] Yastrebov, Anciaux, Molinari, *Tribol. Lett.* 56 (2014)
[3] Dapp, Müser, *Europhys. Lett.* 109 (2015)

Thank you for your attention!

<vladislav.yastrebov@mines-paristech.fr> www.yastrebov.fr